2016

Aligning carbon nanofibers in PCL microfibers using microfluidic method: An approach to efficiently improve electrical conductivity and mechanical strength

Mingchang Lu
Iowa State University

Aligning carbon nanofibers in PCL microfibers using microfluidic method: An approach to efficiently improve electrical conductivity and mechanical strength

by

Mingchang Lu

A thesis submitted to the graduate faculty

in partial fulfillment of the requirements for the degree of

MASTER OF SCIENCE

Major: Mechanical Engineering

Program of Study Committee:
Reza Montazami, Co-Major Professor
Nastaran Hashemi, Co-Major Professor
Chenxu Yu

Iowa State University

Ames, Iowa

2016

TABLE OF CONTENTS

Page

ACKNOWLEDGMENTS iv

ABSTRACT v

CHAPTER 1 INTRODUCTION 1

1.1 Background 1
1.2 References 5

CHAPTER 2 LITERATURE REVIEW 9

2.1 Intrinsically Conductive Polymer Fibers 9
2.2 Polymer Fibers with Conductive Coatings 11
2.3 Conductive fillers/Polymer Composite Fibers 14
2.3.1 Conductive composite fiber spun via electrospinning 15
2.3.2 Conductive composite fiber spun via melt spinning 18
2.3.3 Conductive composite fiber spun via solution spinning 20
2.3.4 Conductive composite fiber spun via other methods 21
2.4 Microfluidic Fiber Fabrication 22
2.4.1 Microfluidics 22
2.4.2 Manufacturing of microchannel 22
2.4.1 Microfluidics 22
2.4.2 Manufacturing of microchannel 22
2.4.2.1 Micromachining 23
2.4.2.2 Soft lithography 23
2.4.2.3 Other methods 24
2.4.3 Fiber fabrication using microfluidic method 24
2.4.4 Composite fiber fabrication using microfluidic method 30
2.5 References 33

CHAPTER 3 FABRICATION OF MOLDS AND MICROCHANNEL 40
3.1 Fabrication of Molds for Microchannel 42
3.2 Fabrication of Microchannel by Molding Replication 49
3.3 References 50

CHAPTER 4 MICROFLUIDIC FABRICATION OF ELECTRICALLY CONDUCTIVE CNF/PCL COMPOSITE FIBER 51
4.1 Experimental Section 51
4.1.1 Materials 51
4.1.2 Preparation of Core and Sheath Solutions 51
4.1.3 Microfluidic Fiber Fabrication 52
4.1.4 Characterization 54
4.2 Results and Discussion 55
4.2.1 Morphology 55
4.2.2 Electrical conductivity 60
4.2.3 Tensile properteis 67
4.3 References 71

CHAPTER 5 CONCLUSION AND FUTURE WORK 72

5.1 Conclusion 72
5.2 Future Work 73
5.3 References 75

ACKNOWLEDGMENTS

I would like to thank my major professor, Reza Montazami, co-major Professor Nastaran Hashemi, and my committee member, Chenxu Yu, for their guidance and support throughout the course of this research.

In addition, I would also like to thank my friends, colleagues, the department faculty and staff for making my time at Iowa State University a wonderful experience.

ABSTRACT

In this thesis work, electrically conductive CNF/PCL composite fibers were fabricated using the microfluidic method. The fibers were made with different content levels of CNFs and flow rate ratios between the core and sheath fluids. The electrical conductivity and tensile properties of these fibers were then investigated.

A cross-flow geometry microfluidic channel with four chevron-shaped grooves as shaping elements was designed for microfluidic fiber fabrication. A CNC micro-milling machine was used to create the PMMA master molds, the surfaces of which were further smoothened by chloroform vapor. PDMS microchannel was prepared by molding replication based on the micro-machined PMMA master molds.

Using the as-fabricated PDMS microchannel, electrically conductive CNF/PCL composite fibers were successfully fabricated using the microfluidic method. It was found that at a CNF concentration of 3 wt.%, the electrical conductivity of the composite fiber increased to 1.11 S/m, which was around 10^{15} times of the electrical conductivity of the pure PCL. The yield strength, Young's Modulus and ultimate strength of the 3 wt.% CNF/PCL composite fiber increased relative to the pure PCL fiber by a factor of 1.72, 2.88, and 1.23, respectively. Further increasing the content of CNF, the electrical conductivity increased slightly, while the tensile strength dropped sharply due to the agglomeration of CNF. Additionally, the results showed that the microfluidic could be considered as an effective method to align CNFs along the fiber in the longitudinal direction. The alignment of the CNFs showed a positive effect on the electrical conductivity and tensile strength.

CHAPTER I

INTRODUCTION

1.1 Background

In recent years, electrically conductive polymer fibers have been extensively investigated due to their promising applications in a wide range of areas, such as static charge dissipation and dust-free clothing [1], sensors [2-6], actuators [7], fiber based wearable electronics [8], energy storage [9], drug release [10], tissue engineering [11], electromagnetic interference shielding [12], and so on.

In general, there are three approaches being used to fabricate electrically conductive polymer fibers: directly spinning of intrinsically conductive polymers, coating insulating polymer fibers with electrically conductive materials to form the conductive network on the surface of the fibers, and fabrication of electrically conductive fillers/polymer composite fibers.

1) The spinning of intrinsically conductive polymer (ICP).

Intrinsically conductive polymers (ICP), such as such as poly(aniline), poly(pyrrole), poly(acetylene) and other conjugated polymers, have been considered as a promising substitute materials for semiconductors or metallic conductors in some special areas owing to their excellent electrical properties compared with general polymers [13, 14]. Electrically conductive polymer fibers could be fabricated by directly spinning of intrinsically conductive polymers via common spinning techniques [15]. However, the spinning process of ICPs is generally very difficult due to their inherent infusibility and insolubility in common solvents [16]. To make a less difficult ICP spinning solution, some toxic or corrosive solvents have been used [15, 17, 18]. Also completed spinning equipment might be needed due to the poor stretchability of the ICP

solution [15]. Additionally, the rigid molecular backbones of conductive polymers result in poor toughness and mechanical brittleness, which restrict the wide application of fibers spun from intrinsically conductive polymers [19, 20].

2) Electrically conductive coating

To avoid the processing difficulties and mechanical brittleness of intrinsically conductive polymer fibers, an alternative way is to coat commercially available fibers or yarns with conductive materials [21]. The conductive coating could significantly increase the conductivity of polymer fibers. Meanwhile, the flexibility and other mechanical properties of polymer fibers can be maintained to some extent. ICPs, carbon nanotubes/polymer composites and other conductive materials have been reported to have been successfully coated onto non-conductive polymer fibers [22-27].However, as scratch and wear resistance of the conductive coatings might be poor, the coated conductive fibers are concerned about their reliability for long-term service owing to the loss of the conductive coatings on the surface [28].

3) Conductive fillers/polymer composite fibers

Conductive fillers/polymer composite fibers have been paid much attention due to the diversity and flexibility of their spinning methods and service reliability. A variety of materials, such as metal filament [29], carbon black [30], intrinsically conductive polymer [31], graphite [23], carbon nanotubes [32, 33], carbon nanofiber [34], have been successfully incorporated into polymer matrix to fabricate conductive composite fibers. In order to significantly increase the conductivity of the insulating polymer matrix, the concentration of the conductive fillers should be above the percolation threshold, at which conductive network is formed by the conductive fillers. In addition to high electrical conductivity, optimal conductive fillers should have fairly

large aspect ratio and can be dispersed in the polymer matrix uniformly, which could favor the formation of conductive network and decrease the percolation threshold [35, 36].

A variety of conventional fiber spinning techniques, including electrospinning [32], wet-spinning [26], and melt spinning [23]have been widely reported to be used to fabricate conductive polymer composite fibers. Microfluidics, on the other hand, has shown promising potentials to be used in a wide scope of applications ranging from energy to biomedical industries [37-42]. Regarding fiber fabrication, the newly emerging microfluidic method has attracted a significant amount of attention by cause of its relatively cheap tooling costs, low consumption of materials, and ability to control the cross-sectional shape and size of the resulting fibers[43]. Owing to the flexibility of the microfluidic approach, a few studies have been published about microfluidic fabrication of polymer composite fibers, into which cells, liquid crystals and gold nanoparticles were incorporated [44-49]. However, to the extent of our knowledge, there has been no research reported on the fabrication of electrically conductive polymer composite fibers based on a microfluidic platform.

In this thesis work, a cross-flow geometry microfluidic channel with four chevron-shaped grooves as shaping elements was designed for microfluidic fiber fabrication. Two polymethylmethacrylate (PMMA) master molds for fabricating the microfluidic channel were made by machining of PMMA substrates using a computer numerical control (CNC) micro-milling machine. Then the polydimethylsiloxane (PDMS) microfluidic channel with three inlets was made via molding replication using the micro-machined PMMA master molds. After that, polycaprolactone (PCL), which is a biocompatible and biodegradable polymer was selected as polymer matrix. Carbon nanofiber (CNF) with high electrical conductivity and large aspect ratio was selected as the electrically conductive filler. Electrically conductive CNF/PCL composite

fibers were fabricated using the microfluidic approach for the first time. The morphology, electrical conductivity, and tensile properties of the resulting fibers fabricated with different content levels of CNF and sheath-to-core flow rate ratios were investigated.

1.2 References

[1] H. Deng, T. Skipa, E. Bilotti, R. Zhang, D. Lellinger, L. Mezzo, Q. Fu, I. Alig, T. Peijs, Preparation of High-Performance Conductive Polymer Fibers through Morphological Control of Networks Formed by Nanofillers, Advanced Functional Materials 20(9) (2010) 1424-1432.

[2] S. Seyedin, J.M. Razal, P.C. Innis, A. Jeiranikhameneh, S. Beirne, G.G. Wallace, Knitted Strain Sensor Textiles of Highly Conductive All-Polymeric Fibers, ACS Applied Materials & Interfaces 7(38) (2015) 21150-21158.

[3] T. Bera, Y. Mohamadou, K. Lee, H. Wi, T. Oh, E. Woo, M. Soleimani, J. Seo, Electrical Impedance Spectroscopy for Electro-Mechanical Characterization of Conductive Fabrics, Sensors 14(6) (2014) 9738.

[4] C. Cochrane, M. Lewandowski, V. Koncar, A Flexible Strain Sensor Based on a Conductive Polymer Composite for in situ Measurement of Parachute Canopy Deformation, Sensors 10(9) (2010) 8291.

[5] C. Li, E.T. Thostenson, T.-W. Chou, Sensors and actuators based on carbon nanotubes and their composites: A review, Composites Science and Technology 68(6) (2008) 1227-1249.

[6] K. Cherenack, C. Zysset, T. Kinkeldei, N. Münzenrieder, G. Tröster, Woven Electronic Fibers with Sensing and Display Functions for Smart Textiles, Advanced Materials 22(45) (2010) 5178-5182.

[7] B. Qi, W. Lu, B.R. Mattes, Strain and Energy Efficiency of Polyaniline Fiber Electrochemical Actuators in Aqueous Electrolytes, The Journal of Physical Chemistry B 108(20) (2004) 6222-6227.

[8] W. Zeng, L. Shu, Q. Li, S. Chen, F. Wang, X.-M. Tao, Fiber-Based Wearable Electronics: A Review of Materials, Fabrication, Devices, and Applications, Advanced Materials 26(31) (2014) 5310-5336.

[9] L. Bao, X. Li, Towards Textile Energy Storage from Cotton T-Shirts, Advanced Materials 24(24) (2012) 3246-3252.

[10] M.R. Abidian, D.H. Kim, D.C. Martin, Conducting-Polymer Nanotubes for Controlled Drug Release, Advanced Materials 18(4) (2006) 405-409.

[11] L. Ghasemi-Mobarakeh, M.P. Prabhakaran, M. Morshed, M.H. Nasr-Esfahani, H. Baharvand, S. Kiani, S.S. Al-Deyab, S. Ramakrishna, Application of conductive polymers, scaffolds and electrical stimulation for nerve tissue engineering, Journal of Tissue Engineering and Regenerative Medicine 5(4) (2011) e17-e35.

[12] S. Shinagawa, Y. Kumagai, K. Urabe, Conductive Papers Containing Metallized Polyester Fibers for Electromagnetic Interference Shielding, Journal of Porous Materials 6(3) (1999) 185-190.

[13] D. Kumar, R.C. Sharma, Advances in conductive polymers, European Polymer Journal 34(8) (1998) 1053-1060.

[14] C. Cochrane, V. Koncar, M. Lewandowski, C. Dufour, Design and Development of a Flexible Strain Sensor for Textile Structures Based on a Conductive Polymer Composite, Sensors 7(4) (2007) 473.

[15] Y. Zhang, G.C. Rutledge, Electrical Conductivity of Electrospun Polyaniline and Polyaniline-Blend Fibers and Mats, Macromolecules 45(10) (2012) 4238-4246.

[16] R. Gangopadhyay, A. De, Conducting Polymer Nanocomposites: A Brief Overview, Chemistry of Materials 12(3) (2000) 608-622.

[17] A. Andreatta, Y. Cao, J.C. Chiang, A.J. Heeger, P. Smith, Electrically-conductive fibers of polyaniline spun from solutions in concentrated sulfuric acid, Synthetic Metals 26(4) (1988) 383-389.

[18] A. Andreatta, S. Tokito, P. Smith, A.J. Heeger, High Performance Fibers of Conducting Polymers, Molecular Crystals and Liquid Crystals Incorporating Nonlinear Optics 189(1) (1990) 169-182.

[19] Y. Zhang, Electrospun nanofibers with tunable electrical conductivity, Department of Chemical Engineering, Massachusetts Institute of Technology, 2013.

[20] L. Nyholm, G. Nyström, A. Mihranyan, M. Strømme, Toward Flexible Polymer and Paper-Based Energy Storage Devices, Advanced Materials 23(33) (2011) 3751-3769.

[21] M. Stoppa, A. Chiolerio, Wearable Electronics and Smart Textiles: A Critical Review, Sensors 14(7) (2014) 11957.

[22] Y. Ding, M.A. Invernale, G.A. Sotzing, Conductivity Trends of PEDOT-PSS Impregnated Fabric and the Effect of Conductivity on Electrochromic Textile, ACS Applied Materials & Interfaces 2(6) (2010) 1588-1593.

[23] B. Kim, V. Koncar, E. Devaux, C. Dufour, P. Viallier, Electrical and morphological properties of PP and PET conductive polymer fibers, Synthetic Metals 146(2) (2004) 167-174.

[24] D. Knittel, E. Schollmeyer, Electrically high-conductive textiles, Synthetic Metals 159(14) (2009) 1433-1437.

[25] T. Bashir, L. Fast, M. Skrifvars, N.-K. Persson, Electrical resistance measurement methods and electrical characterization of poly(3,4-ethylenedioxythiophene)-coated conductive fibers, Journal of Applied Polymer Science 124(4) (2012) 2954-2961.

[26] P. Xue, K.H. Park, X.M. Tao, W. Chen, X.Y. Cheng, Electrically conductive yarns based on PVA/carbon nanotubes, Composite Structures 78(2) (2007) 271-277.

[27] C. Robert, J.F. Feller, M. Castro, Sensing Skin for Strain Monitoring Made of PC–CNT Conductive Polymer Nanocomposite Sprayed Layer by Layer, ACS Applied Materials & Interfaces 4(7) (2012) 3508-3516.

[28] D.D.L. Chung, Electromagnetic interference shielding effectiveness of carbon materials, Carbon 39(2) (2001) 279-285.

[29] Y. Zhu, Y. Zhao, X. Zhang, L. Wang, X. Wang, J. Zhang, P. Han, J. Qiao, Metal filaments/nano-filler filled hybrid polymer fibers with improved conductive performance, Materials Letters 173 (2016) 26-30.

[30] J.X.X.C.Y.C.X. Chun, Non-continuous Conductive Behavior of CB/PET Fiber, Chinese Journal of Materials Research 24(3) (2010) 311-314.

[31] B. Zhang, T. Xue, J. Meng, H. Li, Study on property of PANI/PET composite conductive fabric, The Journal of The Textile Institute 106(3) (2015) 253-259.

[32] J.S. Jeong, J.S. Moon, S.Y. Jeon, J.H. Park, P.S. Alegaonkar, J.B. Yoo, Mechanical properties of electrospun PVA/MWNTs composite nanofibers, Thin Solid Films 515(12) (2007) 5136-5141.

[33] A.-T. Chien, P.V. Gulgunje, H.G. Chae, A.S. Joshi, J. Moon, B. Feng, G.P. Peterson, S. Kumar, Functional polymer–polymer/carbon nanotube bi-component fibers, Polymer 54(22) (2013) 6210-6217.

[34] R. Jain, H.G. Chae, S. Kumar, Polyacrylonitrile/carbon nanofiber nanocomposite fibers, Composites Science and Technology 88 (2013) 134-141.

[35] Y. Yu, S. Song, Z. Bu, X. Gu, G. Song, L. Sun, Influence of filler waviness and aspect ratio on the percolation threshold of carbon nanomaterials reinforced polymer nanocomposites, Journal of Materials Science 48(17) (2013) 5727-5732.

[36] J.Y. Yi, G.M. Choi, Percolation behavior of conductor-insulator composites with varying aspect ratio of conductive fiber, Journal of electroceramics 3(4) (1999) 361-369.

[37] D. Sinton, Energy: the microfluidic frontier, Lab on a Chip 14(17) (2014) 3127-3134.

[38] S.M. Mitrovski, L.C. Elliott, R.G. Nuzzo, Microfluidic devices for energy conversion: Planar integration and performance of a passive, fully immersed H2-O2 fuel cell, Langmuir 20(17) (2004) 6974-6976.

[39] F. Sharifi, S. Ghobadian, F.R. Cavalcanti, N. Hashemi, Paper-based devices for energy applications, Renewable and Sustainable Energy Reviews 52 (2015) 1453-1472.

[40] F. Sharifi, Z. Bai, R. Montazami, N. Hashemi, Mechanical and physical properties of poly(vinyl alcohol) microfibers fabricated by a microfluidic approach, RSC Advances 6(60) (2016) 55343-55353.

[41] F. Sharifi, D. Kurteshi, N. Hashemi, Designing highly structured polycaprolactone fibers using microfluidics, Journal of the Mechanical Behavior of Biomedical Materials 61 (2016) 530-540.

[42] P.J. Goodrich, F. Sharifi, N. Hashemi, Rapid prototyping of microchannels with surface patterns for fabrication of polymer fibers, RSC Advances 5(87) (2015) 71203-71209.

[43] Z. Bai, J.M. Mendoza Reyes, R. Montazami, N. Hashemi, On-chip development of hydrogel microfibers from round to square/ribbon shape, Journal of Materials Chemistry A 2(14) (2014) 4878-4884.

[44] B.R. Lee, K.H. Lee, E. Kang, D.-S. Kim, S.-H. Lee, Microfluidic wet spinning of chitosan-alginate microfibers and encapsulation of HepG2 cells in fibers, Biomicrofluidics 5(2) (2011) 022208.

[45] Y. Jun, M.J. Kim, Y.H. Hwang, E.A. Jeon, A.R. Kang, S.-H. Lee, D.Y. Lee, Microfluidics-generated pancreatic islet microfibers for enhanced immunoprotection, Biomaterials 34(33) (2013) 8122-8130.

[46] Y. Zuo, X. He, Y. Yang, D. Wei, J. Sun, M. Zhong, R. Xie, H. Fan, X. Zhang, Microfluidic-based generation of functional microfibers for biomimetic complex tissue construction, Acta Biomaterialia 38 (2016) 153-162.

[47] A.R. Shields, C.M. Spillmann, J. Naciri, P.B. Howell, A.L. Thangawng, F.S. Ligler, Hydrodynamically directed multiscale assembly of shaped polymer fibers, Soft Matter 8(24) (2012) 6656-6660.

[48] D.A. Boyd, J. Naciri, J. Fontana, D.B. Pacardo, A.R. Shields, J. Verbarg, C.M. Spillmann, F.S. Ligler, Facile Fabrication of Color Tunable Film and Fiber Nanocomposites via Thiol Click Chemistry, Macromolecules 47(2) (2014) 695-704.

[49] M. Hu, R. Deng, K.M. Schumacher, M. Kurisawa, H. Ye, K. Purnamawati, J.Y. Ying, Hydrodynamic spinning of hydrogel fibers, Biomaterials 31(5) (2010) 863-869.

CHAPTER 2

LITERATURE REVIEW

2.1 Intrinsically Conductive Polymer Fibers

Owing to their low density, corrosion resistance and excellent electrical property which is comparable to semi-conductors or even metals, intrinsically conductive polymers (ICP) including polyaniline, polypyrrole, polyacetylene and polythiophene have been paid much attention since the discovery [1-5].

Electrically conductive fibers could be obtained by spinning of ICPs using commercially available fiber spinning techniques. However, due to the inherent infusibility and insolubility in general solvents, conductive polymers are generally difficult to be spun into fiber directly.

To increase the solubility, one approach is to chemically modify the ICPs, such as grafting polymer chains and synthesizing copolymers. However, chemical modification of the molecular structure could also decrease the conductivity of the ICPs [6].

In order to make a spinnable solution of ICPs without chemical modification, some special solvents have been used.

Andreattta et al. successfully dissolved polyaniline (PANI) into concentrated sulfuric acid [7]. The resulting polyaniline/sulfuric acid solution was spun into PANI monofilaments using dry-jet wet spinning. Although the mechanical properties of the as-spun PANI fiber were relatively weak, an excellent conductivity of up to 20-60 S/cm was obtained which might be ascribed to the high degree of crystallinity proved by wide-angle X-ray diffraction. To improve the mechanical properties of the resulting PANI fiber, the mixture of poly-(p-phenylene terephthalamide) (PPTA) and PANI was dissolved in concentrated sulfuric acid for fiber

fabrication [8]. The mechanical properties were improved significantly due to the addition of PPTA. Meanwhile, Incorporation of PPTA did not lead to a large decrease in the electrical conductivity.

Pomfret et al. made a spinnable solution by dissolving 2-acrylamido-2-methyl-1-propanesulfonic acid protonated PANI into dichloroacetic acid [9]. The PANI fibers were obtained by wet-spinning of the PANI solution. In addition to good mechanical properties, the electrical conductivity of the as-spun fiber was 150 S/cm. Also, it was found that the drawing of the PANI fibers could lead to increasing of both mechanical properties and electrical conductivity, which might be due to the stretching induced alignment of the PANI molecular chains.

Instead of making spinnable solution using ICPs directly, an alternative way is to use a solution of ICP precursors, which show better solubility than ICPs. After fiber spinning, post-process is required to convert precursor polymers to conjugated polymers.

Andreattta et al.[8] fabricated poly(2,5-dimethyoxy-p-phenylene vinylene) (PDMPV) precursor and poly(2,5-thienylene vinlene) (PTV) precursor fibers using PDMPV/chloroform and PTV/chloroform solution via solution spinning approach. After the drawing process, the precursor fibers were converted to PDMPV and PTV fibers by doping with iodine vapor. The mechanical properties and electrical conductivity showed increasing upon drawing. Although the iodine vapor doping slightly decreased the mechanical strength, the PDMPV and PTV precursors could be converted to PMDPV and PTV fibers, which exhibited high electrical conductivity.

Additionally, the fairly rigid molecular backbones of ICPs general endow the ICPs solution poor elasticity, which makes it difficult to fabricate ICPs using some commercially available spinning techniques, like electrospinning [10].

To address the insufficient elasticity of PANI solution, a co-axial electrospinning equipment was used for electrospinning of PANI by Zhang et al. [11]. The coaxial electrospinning system was consisted of two concentric spinnerets. During the electrospinning process, the low-elasticity PANI solution and high-elasticity poly(methyl methacrylate) (PMMA) were introduced into the core spinneret and outer spinneret respectively. The spinning of the PANI core solution into continuous fiber was achieved owing to the elongation induced by high-elasticity PMMA shell solution. Pure PANI fiber was obtained by washing away PMMA shell of the electrospun core-shell fiber with isopropanol. The PANI fiber showed the conductivity of 50 ± 30 S/cm, which could be further increased to 130 ± 40 S/cm through aligning of polymer chains achieved by solid-state drawing.

In summary, polymer fibers with excellent electrical conductivity could be obtained by directly spinning of ICPs. However, to achieve spinning of ICPs, strongly corrosive or toxic solvent, complex spinning equipment or post-processing procedures might be needed. Also, due to the fairly rigid molecular backbones of ICPs, ICP fibers generally exhibit considerably mechanical brittleness, which restricts their application in some areas [12].

2.2 Polymer Fibers with Conductive Coatings

Coating commercially available fibers with conductive materials is a relatively convenient and effective approach to endow fibers with fairly high electrical conductivity. At the same time, the mechanical properties of the coated fibers could be retained.

One of the widely used coating materials is intrinsically conductive polymer because of their high electrical conductivity, environmental resistance and ease of synthesis [13].

Ding et al. successfully coated Spandex, cotton, polyester and other commercially available fabric with poly(3,4-ethylenedioxythipphene) polystyrene sulfonate (PEDOT-PSS) nanoparticles by simply immersion of the fabric into the PEDOT-PSS aqueous suspension [14]. Not only the electrical conductivity was increased significantly, the stretchability of the fabric was also retained. In addition, it was found that more immersion times and using fabric with higher water uptake could result in higher conductivity.

As mentioned in the previous section, intrinsically conductive polymers are generally non-soluble in most of the solvents, special treatment is needed before making ICP solutions.

Kim et al. increased the solubility and dispersion of PANI in xylene via dodecylbenzene sulfonic acid (DBSA) treatment and used the as-prepared PANI/xylene solution as the bath for coating polyethylene terephthalate (PET) fibers [15]. Compared with PANI filled composite fibers from melt spinning, the PANI-coated PET fibers showed higher conductivity and better mechanical properties. Additionally, the conductivity of the coated fibers was significantly influenced by the coating temperature and duration time, surface properties of fibers before coating, and soak-up speed of the fibers.

Another way to address the difficulty of dissolving intrinsically conductive polymers is to coat fibers with ICP monomers which would be further polymerized into polymers on the surface of the fibers.

PANI coated PET conductive fibers with highly improved conductivity were prepared via processing PET fibers through immersion into NaOH solution, washing with DI water, plasma treatment, immersion in aniline solution and oxidative polymerization [16]. The treatment of PET fibers with NaOH and plasma turned out to be an effective method to produce projections and pits on the surface of PET fiber, which could play a role in fixing the PNAI coating. The

reliability of the conductive PNAI coating was also investigated by washing PANI coated PET fibers with ultrasonication cleaner. The surface resistivity increased from around 170 Ohm to 1450 Ohm after five times of washing. Besides, although the pre-treatment produced rough surface could increase the bonding between PET fibers and PANI coating, the mechanical properties were decreased due to the resulting defects.

Kim et al. successfully coated Polypyrrole (PPy) on the surface of the PET fibers via polymerization of pyrrole on the surface of the substrate PET fibers [17]. Firstly, pyrrole aqueous solution containing polyvinyl alcohol (PVA) as the surfactant was sprayed on the surface of PET fibers. Then the spraying of oxidant solution was followed. The chemical polymerization of pyrrole was performed at certain temperatures with desired time. After repeating the chemical polymerization for several times, electrochemical polymerization was followed in an electrolyte solution. It was found that the electrical conductivity of the PPy/PET fibers could be increased by electrochemical polymerization, which produced more uniform and thicker PPy layer on the surface of PET substrate fiber. Also, to achieve a uniform coating on the substrate fiber, polymerization parameters and concentration of the monomer solution should be optimized.

Besides, monomer ethylenedioxythiophene (EDOT) was also reported to be coated on various commercially available polymer fibers [13, 18, 19]. After polymerization process, PEDOT conductive layer was formed on the surface of the substrate fibers.

In addition to using conductive polymers as coating materials, carbon nanotubes have also been paid much attention in this area.

Polyelectrolyte-based carbon nanotubes (CNTs) coating was successfully produced on the surface of cotton yarn after immersing cotton yarn into CNTs suspension [20]. The as-prepared cotton fibers possessed satisfied electrical conductive which was enough to be used in a

simple LED circuit. Owing to the interaction between polyelectrolyte and cotton substrate fiber, the CNTs showed irremovable from the substrate fiber upon exposure to heat and solvents. Additionally, CNTs coating not only increased the conductivity of the cotton fiber, but also improved the mechanical properties significantly.

Xue et al. dipped five kinds of commercially available fibers into CNTs and PVA (1:1) solution to fabricate coated conductive fibers [21]. The resulting CNT-coated fibers showed low resistivities ranging from 0.25 Kohm/cm to 48.67 Kohm/cm. The mechanical strength and flexibility of the substrate fibers were also retained.

Robert et al. deposited CNTs/polymer composite on the surface of PET fibers via spraying CNTs/polymer solution on PET fibers layer by layer. Owing to the preserved flexibility and tunable electrical parameters by adjusting coating layers and CNTs concentration, the as-prepared fibers were made into a smart monitor of strain [22].

In summary, coating insulating polymer fibers with conductive material is a relatively simple method for making highly electrically conductive fibers. The conductive coating could increase the conductive significantly and preserve or even enhance the mechanical properties of the original fibers. However, special methods are required to increase the stability and reliability of the conductive coatings.

2.3 Conductive Fillers/Polymer Composite Fiber

In order to bypass the difficulties of spinning of ICPs and improving the stability and reliability of conductive coatings, great efforts have been devoted to fabricating electrically conductive fillers/polymer composite fibers. To achieve significantly increasing of electrical

conductivity, the concentration of the conductive fillers should be above the percolation threshold, at which the conductive network is formed by the fillers in the polymer matrix.

2.3.1 Conductive composite fiber spun via electrospinning

As a widely used fiber fabrication technique, electrospinning is to utilize electric force to produce polymer fibers with the diameters of ranging from nanometers to microns. Generally, there are two types of electrospinning set up, i.e. vertical and horizontal set up, both of which contains three main parts: a high voltage power source, spinneret and fiber collecting part [23]. The process of electrospinning is [24]: (1) high voltage is applied between spinneret and fiber collector; (2) the polymer solution or molten polymer is pumped into the spinneret; (3) at the critical point, a Taylor cone will form because of the voltage power is high enough to produce electrostatic force to overwhelm the surface tension of the spinnable liquid; (4) the fiber jet will emit from the apex of the Taylor cone and travel further to the collector.

The advantages of electrospinning are low-cost setting up, flexibility, feasibility for various kinds of polymers, and probability for mass production. However, the application of electrospinning is limited by the complexity of controlling of fiber alignment and difficulty of producing single continuous fiber [25].

Regarding fabrication of composite fibers, it is worth noting that the electrospinning is considered to have the capability of aligning the fillers with aspect ratio larger than 1 in polymer matrix due to the severe stretching during spinning process [26].

Jeong et al. performed electrospinning of multi-walled carbon nanotube (MWCNT)/polyvinyl alcohol (PVA) composite fiber using suspension of acid-modified MWCNT in PVA aqueous solution [27]. Due to the hydrophobicity of the CNT surface, the

dispersed MWCNTS could be wrapped by the PVA molecules driven by the thermodynamic force [28]. The resulting composite fibers with the lower concentration of MWCNTs exhibited smooth surface, uniform morphology and increased mechanical properties. However, the higher concentration of carbon nanofiber resulted in rough surfaces, defects, distortion and decreased mechanical strength of the composite fiber due to the agglomeration of MWCNTs. In addition to the viscosity of the spinnable solution, the dispersion of MWCTs in polymer solution could also affect the fluid charge density which plays a significant role in the electrospinning process, formation and properties of the final fiber products.

The uniformity of dispersion and alignment of conductive fillers along the axial direction of the composite fiber is beneficial for mechanical reinforcement and formation of the conductive network [29].

Salalha et al. successfully fabricated single-walled carbon nanotubes (SWCNTs)/ poly (ethylene oxide) PEO composite fibers via electrospinning of SWCNTs suspension in PEO/(ethanol/water) solution containing amphiphilic polymer as the surfactant [30]. It was found that the distribution and alignment of the carbon nanofiber inside the as-spun composite fibers are highly affected by the CNTs-polymer interaction and dispersion uniformity of CNTs in polymer solution before electrospinning.

Kedem et al. performed electrospinning using the suspension of CNTs in poly(acrylonitrile) (PAN)/dimethylformamide (DMF) solution. HRSEM and TEM images showed that CNTs were uniformly dispersed and highly orientated in the PAN matrix [31].

Sundaray et al. prepared MWCNT/PMMA composite fibers via electrospinning of MWCNTs suspension in PMMA/chloroform solution. The as-spun composite fiber showed very low percolation threshold (addition of 0.05 wt.% increased the conductivity from 10^{-12} S/m to 4.5

$\times 10^{-3}$ S/m), which might be due to the uniformly dispersed and uniaxial aligned MWCNTs in PMMA matrix [32].

In addition to carbon nanotubes, other conductive materials could also be used as conductive fillers. Due to the challenge of spinning of intrinsically conductive polymers as mentioned in the previous section, they could also be used as conductive fillers for spinnable polymers to fabricate conductive composite fibers.

Ghasemi-Mobarakeh et al. blended PANI with PCL/gelation (70:30) solution, which was further used for electrospinning [33]. The incorporation of PANI led to the enhancement of mechanical properties and electrical conductivity. Additionally, the incorporation of PANI showed decreasing of fiber diameter, which might be due to the increasing of fluid charge density.

In summary, as a simple and widely used spinning techniques, electrospinning turned out to be an effective approach for fabricating electrically conductive composite fibers. The severe stretching during electrospinning could lead to the orientation of conductive fillers with high aspect ratio, which facilitates the reinforcement of mechanical properties and formation of the conductive network at lower filler concentration. Despite the change of viscosity and elasticity, the addition of conductive fillers could also change the fluid charge density, which significantly affects the electrospinning. Also, producing single continuous fiber and controlling the alignment of the fibers remain as challenges for electrospinning.

2.3.2 Conductive composite fiber spun via melt spinning

Another widely used fiber spinning technique is melt spinning. During melt spinning process, the formation of polymer fibers is achieved via cooling of molten polymer which comes through a spinneret driven by the stress field.

Kim et al. used PANI-ES, PPy and graphite spherical nanoparticles as conductive fillers for LDPE and PP separately to fabricate electrically conductive fiber via melt spinning [15]. Due to poor dispersion and discontinuous connection of conductive fillers in the polymer matrix, the conductivity of the composite fiber was unsatisfactory even at a filler content level of 30 wt.%. It was concluded that extra mixing process was required to ensure uniform dispersion of fillers in the polymer matrix.

Instead of using one type of conductive filler, the mixture of conductive fillers with different shapes or aspect ratios might be able to facilitate the formation of the conductive network in the polymer matrix.

The mixture of conductive fillers of silver particles and carbon nanotubes were embedded into polypropylene to fabricate conductive composite fiber via melt spinning [34]. It was demonstrated that the CNTs played a role in bridging silver particles to form conductive network at lower filler concentration. Although fibers spun from melt spinning generally have better mechanical properties than fibers spun from other spinning methods, it was presented that several obstacles need to be overcome to fabricate composite fiber using melt spinning: a. the difficulty of processing liquid with low viscoelasticity and high viscosity owing to the addition of conductive fillers; b. uniform dispersion conductive fillers into the polymer matrix; c. crystallization of polymer matrix induced by the nucleation effect of fillers.

Single-wall carbon nanotubes(SWNTs) were mixed with poly(methyl methacrylate (PMMA) to be fabricated into composite fibers using melt spinning method [35]. The incorporation of SWNTs in PMMA fiber resulted in rough surfaces, non-uniform diameter along the axial direction and improved mechanical properties. To investigated the influence of melt spinning process on the alignment of SWNTs in PMMA matrix, SWNTs/PMMA composite film was prepared and characterized. It was concluded that the SWNTs could be oriented along the fiber axial direction based on polarized resonant Raman spectroscopy results and higher electrical conductivity of composite films along flow direction(11.5 S/m with 6.6 wt.% of SWNTs) than along the direction perpendicular to the flow (7.0 S/m with 6.6 wt.% of SWNTs)

Fornes et al. uniformly dispersed SWNTs and MWNTs into polycarbonate by solvent blending and melt compounding [36]. The resulting CNT/polycarbonate composites were spun into fibers via melt spinning. It was concluded that increasing the draw ratio during melt spinning could improve the orientation of the CNTs due to the increased elongational stress applied on CNTs.

In general, the electrical conductivity of conductive filler/polymer composite would decrease upon stretching due to the disconnection of the conductive fillers. To address this problem, Zhu et al. fabricated low melting point alloy (LMPA)/ polypropylene composite fibers using melt spinning [37]. At a temperature between melting points of LMPA and polypropylene, the conductivity of the composite fibers increased owing to the building of denser conductive network by the conversion of LMPA particles to filaments under stretching stress.

In summary, electrically conductive filler/polymer composite fiber could also be fabricated using melt spinning technique. To achieve uniform dispersion of CNTs in polymer matrix, severe mechanical stirring, ultrasonication and solvent-aided mixing might be needed.

Also, the blending of CNTs with polymer matrix would increase the viscosity and decrease the viscoelasticity, which could influence the melt spinning process. In addition, the conductive fillers could also play a role as nuclei and affect the crystallization of crystallizable polymer matrix.

2.3.3 Conductive composite fiber spun via solution spinning

For solution spinning, the spinnable liquid is made from polymer solution. Based on the solidification approach, solution spinning could be further divided into two categories: dry spinning and wet spinning. During dry spinning, polymer fibers are solidified due to the evaporation of the solvent induced by the heated inert gas. For wet spinning, the solidification of polymer fibers occurs in a coagulation bath which contains non-solvent of the polymer [38].

Still, the uniform dispersion of conductive fillers plays a great role in increasing the conductivity of composite fibers. Xue et al. fabricated CNT/PVA composite fiber using wet spinning [21]. The resulting composite fiber containing 40 wt.% CNTs still showed a very high electrical resistivity due to the agglomeration of CNTs in the PVA matrix.

Seyedin et al. fabricated conductive composite fibers with polyurethane (PU) as matrix and poly (3, 4-ethylenedioxythiophene):poly(styrenesulfonate) (PEDOT:PSS) as conductive fillers using wet spinning [39]. The composite fibers showed an electrical conductive of up to 9.4 S/cm with 13.5 wt.% of ICP fillers. In addition, the composite fibers showed suitability for knitting textiles because of the excellent mechanical properties.

Ma et al. fabricated highly conductive composite fibers with fair stretchability using wet spinning method [40]. The electrical conductivity of the composite fibers was up to 17460 S/cm. Besides, the fibers possessed high stretchability which exhibited a conductivity of 236 S/cm

under a strain of 490%. The as-spun composite fiber was composited of silver nanoparticles, silver modified multiwall nanotubes (Ag-MWCNTs), ionic liquid (1-butyl-4-methylpyridinium tetrafluoroborate) and poly(vinylidene fluoride-co-hexafluoropropylene) (PVDF-HFP) as the matrix. The Ag nanoparticles could significantly increase the contact area of the conductive fillers. Owing to the high aspect ratio, the Ag-MWCNTs could build a conductive bridge between Ag nanoparticles. The dispersion of Ag-MWCNTs could be improved by the ionic liquid. Also, the ionic liquid could also play a role as the plasticizer, which made it possible to incorporate high concentration levels of CNTs without losing the flexibility of the original polymer matrix [41].

In summary, solution spinning has also been demonstrated as a viable method to fabricate electrically conductive filler/polymer composite fibers. Compared with melt-spinning, the solvent could facilitate the dispersing of fillers in the polymer matrix. Also, it is easier to achieve the required spinning parameters by adjusting the content of solvent.

2.3.4 Conductive composite fiber spun via other methods

Chien et al. used a bi-component fiber spinning equipment fabricated core-shell structured composite fibers with a polyacrylonitrile (PAN) as the outer layer and CNT/PAN composite as the core component or PAN as the core layer and CNT/PAN composite as the outer component via gel-spinning [42]. The resulting fibers contained uniformly dispersed and oriented CNTs in PAN matrix, which endowed the composite fiber with excellent mechanical properties and electrical conductivity of 0.366 S/m.

Deng et al. achieved orientation of CNTs in the polymer matrix through solid-state drawing and annealing [43]. Owing to the orientation of CNTs, the resulting tapes and fibers showed an electrical conductivity of up to 275 S/m with only 0.5 wt% of CNTs incorporated.

Basically, to achieve great enhancement of the electrical conductivity and mechanical properties, the spinning technique should be able to lead the alignment of conductive filler along the fiber longitudinal direction.

2.4 Microfluidic Fiber Fabrication

2.4.1 Microfluidics

The research of microfluidics focuses on investigation and manipulation of fluids at the dimension of submillimeter (microliter or nanoliters) [44]. Through pumping fluids into microfluidic channels with precisely designed patterns [45], the fluid phenomenon, which is greatly different from that at macroscale, could be studied and handled [44]. In addition, microfluidics could also provide the advantages of smaller volume of reagent, shorter reaction time, and possibility of integrating several laboratory experiments on one single chip, referred as “lab-on –a-chip” [46]. Up to now, microfluidics has shown a promising potential to be used to address problems in a variety of fields ranging from biological technology to energy areas [47-51].

2.4.2 Manufacturing of microchannel

The research of microfluidics is based on the microfluidic channels. Currently, several approaches have been used to fabricate microfluidic channels.

2.4.2.1 Micromachining

Micromachining refers to the manufacturing processes that might include cutting, bonding, forming, deforming and removing of materials by using a variety of tools to produce required patterns with the dimension less than 1mm [52]. Micromachining could be performed on a variety of materials as long as the softness and ductility of the materials are suitable for machining [53]. Microchannels made from silicon [54], glass [55], quartz [56], metal [57] and plastic [58] through micromachining have been widely reported. In general, there are two kinds of micromachining: bulk-micromachining and surface-micromachining. For bulk-micromachining, a huge amount of materials would be removed from the substrate [59]. In contrast, for surface-micromachining process, micro structures are formed from deposited thin films [60]. Compared with bulk-micromachining, surface-micromachining wastes fewer materials and requires fewer post-procedures [61].

Compared with other microchannel manufacturing techniques, micromachining could result in fairly high precision which also associated high price, intensive labor, professional skills and expensive equipment [46].

2.4.2.2 Soft lithography

Soft lithographic is a technique of nano- or microfabrication based on self-assembly and molding replication [62]. Generally, the soft lithography is followed by bonding of two layers to form a complete microfluidic device. Owing to its good mechanical properties, transparency and ease of manufacturing, polydimethylsiloxane (PDMS) has been the most widely used material for soft lithography [62]. Soft lithography has the advantages of fast, cheap and suitable for application in biological applications [46].

2.4.2.3 Other methods

As a fast-developing manufacturing technique, 3D printing has also been demonstrated to be able to create microfluidic device [63]. However, the precision and resolution of 3D printing still restrict its application in the area of microfluidic device manufacturing [64].

Through using UV laser photoablation, Roberts et al. produced micro structures on the surface of polystyrene, polycarbonate, cellulose acetate and poly(ethylene terephthalate) [65]. The integrated microchannel was fabricated by bonding of the as-prepared polymer substrates using film lamination technique.

Khoury et al. created microfluidic device directly on a substrate by photo-curing pre-polymer [66]. The shallow cavity on the substrate was used to control the position of the pre-polymer liquid, which was cured and solidified after exposure to UV light. This technique is relatively fast, cheap and no special equipment or skills are required. However, the precision and resolution might be affected by the resolution of the cavity on the substrate and volume change of the pre-polymer after curing.

2.4.3 Fiber fabrication using microfluidic method

Traditional fiber fabrication techniques, including electrospinning, melt-spinning, gel-spinning, wet spinning, dry-spinning, are always associated with extreme processing conditions (high temperature, high voltage, severe shearing, et al.) [67]. In addition, the cross-sectional shape of fibers fabricated from traditional techniques is generally circular due to the surface tension. By contrast, microfluidic fiber fabrication as a newly developed technique could provide mild processing condition, controllable fiber size and various cross-sectional shapes [68]. The mild processing condition makes it possible to incorporate sensitive biological materials, like

cells and proteins into fibers. Also, the adjustable sizes, cross-sectional shapes and microstructures of the fibers are considered to have the promising application in a wide of areas, such as improving mechanical properties of fibers, providing reservoirs for functional materials, guiding the proliferation of cells, and so on. In general, microfluidic fiber fabrication is based on two kinds of flows: core flow and sheath flow. Curable monomer, pre-polymer or polymer solution is used as core flow, which will be polymerized or solidified into fibers. Sheath flow might play a role in applying hydrodynamic focusing on core flow, providing solidification medium for core flow and also separating solidified fibers from the microchannel walls to prevent clogging of the microchannel. Through adjusting built-in shaping features and flow rate ratio, the cross-sectional size and shape could be controlled [69].

The development of microfluidic fiber fabrication is mainly along two directions: microchannel design which includes concentric-flow, cross-flow, and built-in shaping features to achieve 3D hydrodynamic focusing, and fiber solidification method which includes solvent extraction, chemical polymerization and photopolymerization [67].

Kang et al. designed a rectangular concentric-flow micro-device with slit-shaped shaping elements on the bottom of the channel, using which thin flat alginate fibers were fabricated [70]. It was demonstrated that the slit-shaped shaping elements were able to produce engraved patterns on the surface the fibers along the axial direction. Not only the size of the flat fibers but also the shape and size of the engraved patterns could be controlled by simply adjusting the speed ratio of the core flow and sheath flow. After culturing different types of cells on the as-spun fibers, it showed that the engraved patterns were useful for controlling the morphology and alignment of the cells.

A cylindrical concentric-flow microchannel was made by insertion of a pipet into a PDMS platform, using which Poly(L-lactic-co-glycolic acid) (PLGA) fibers were fabricated [71]. PLGA was dissolved in Dimethyl sulfoxide (DMSO) to be used as the core flow and the sheath flow was 1:1 (volume ratio) mixture of glycerin and DI water. As core flow and sheath flow were introduced into the microchannel, the precipitation of PLGA occurred due to the solvent exchange between core flow and sheath flow. The PLGA fiber exhibited highly porous structure in the center and a denser outer layer. Also, the diameter of the PLGA fiber was controllable via changing the speed ratio between core flow and sheath flow. Besides, owing to the mild processing condition, protein was successfully incorporated into the PLGA fiber by using the mixture of PLGA solution and protein solution as core flow.

Cheng et al. devised a cylindrical concentric-flow microchannel with one tapered inlet for core flow and two cylindrical inlets for sheath flow which were mutually perpendicular to each other [72]. This specially designed microchannel was demonstrated to be able to mimic silkworm-spinning. By using the mixture of silk fibroin and alginate solution as core fluid and $CaCl_2$ solution as sheath fluid, the silk fibroin-based hydrogel fiber was obtained.

As the core flow and sheath flow are introduced into the microfluidic channel with a concentric-flow geometry, the core flow would be fully surrounded by the sheath flow which facilitates the hydrodynamic focusing and makes the regulation of fiber diameters simple via adjusting the flow speed ratio. However, it is hard to make fibers with a diameter smaller than 100 um and fabrication of fibers with special cross-sectional shape still remains a challenge using microchannel with a concentric-flow geometry [67].

The microchannel with cross-flow geometry is typically composed of in-plane core and sheath flow sections, between which the angles are specified.

Duboin et al. utilized a “T-junction” microchannel for fabricating microfibers [73]. Through introducing two immiscible polymer aqueous solution and UV-curable pre-polymer solution as sheath flow and core flow respectively, fabrication of diameter-adjustable short polymer fiber was achieved upon UV exposure.

Nunes et al. made a special modification of the general cross-flow geometry by setting a sequence of pillars in the channel as shaping elements [74]. Fibers with a variety of cross-sectional shapes, such as triangular, diamond, and U-shaped were fabricated by simply adjusting the flow rate ratios. What is more attractive is that the experimental results were consistent with the modeling results from U-flow, which would be a useful tool to design microchannel and predict fibers shapes.

As general cross-flow microchannel could only provide in-plane hydrodynamic focusing, some shaping elements are required to produce vertically hydrodynamic focusing.

The typical design is the sheath-flow microchannel with diagonal and chevron-shaped grooves on the top the bottom of the walls [75]. Owing to these grooves, core flow could be surrounded by the sheath flow, which would result in solvent exchange and hydrodynamic focusing. Similar designs have been reported to fabricate gelatin [68], poly(vinyl alcohol) (PVA) [76], and polycaprolactone (PCL) [50]fibers.

There are mainly three methods for solidifying fibers in the microchannel, including solvent extraction or exchange, chemical polymerization and photopolymerization [67].

Generally, to achieve solidification of fibers via solvent extraction, the solvent for core flow should be miscible with the sheath flow solvent, which is not a good solvent for the polymer in core fluid.

Bai et al. fabricated gelatin fibers using gelatin/dimethyl sulfoxide(DMSO) solution as core flow and ethanol as sheath flow [68]. As core fluid and ethanol fluid were introduced into the microchannel, gelatin fibers solidified due to the dissipation of DMSO into ethanol and the insolubility of gelatin in ethanol.

Through carefully selecting solvents for core flow and sheath flow, PMMA, PVA and PCL could also be solidified via solvent extraction [50, 75, 76].

In addition to solidification of fibers via solvent extraction, chemical polymerization inside the microchannel is an alternative approach to achieve solidification of polymer fibers.

Typically, monomer or prepolymer solution is introduced into microchannel as core fluid. The solution of curing agent would be introduced into microchannel as sheath fluid. The sheath flow not only plays a role in hydrodynamic focusing but also providing the curing agent to polymerize or crosslink the pre-polymer in core flow.

Kang et al. achieved fabrication of alginate fibers through solidification induced by chemical polymerization [70]. Calcium chloride solution and alginate solution were introduced into the microchannel as sheath fluid and core fluid respectively. The alginate was crosslinked and solidified as calcium ions in the sheath fluid diffused into core fluid. Additionally, it was found that the properties of the resulting alginate fiber were significantly affected by the concentration of alginate solution, which determined the core fluid viscosity and chemical reaction time.

In general, the fluid passes through the microchannel very fast, and it requires longer time to achieve fiber solidification using chemical polymerization. Photo-polymerization, especially UV- induced polymerization, has been paid much attention to solidifying fibers in microfluidic channel as an alternative method for chemical polymerization. Compared with chemical

polymerization, polymerization initiated by light has advantages of faster reaction speed and easier to control. As the reaction time of the photo-polymerization is very short, the shape of the fiber could be locked immediately after hydrodynamic focusing. By adjusting the strength and exposure time of the light source and exposure location, the photo-polymerization inside the channel could be controlled simply.

Shi et al. performed microfluidic fabrication of UV-curable methacrylamide-modified gelatin (GelMA) fibers through UV initiated polymerization [77]. Owing to the short polymerization and solidification time initiated by UV exposure, the grooved pattern on the surface of resulting fibers could be accurately controlled and locked.

Nunes et al. introduced UV-curable poly(ethylene glycol) diacrylate (PEG-DA) and inert medium into microchannel as core fluid and sheath fluid separately [74]. A variety of accurately controlled cross-sectional shapes could be locked by UV- initiated polymerization as UV source was applied after the shaping section of the channel.

In summary, microfluidic fiber fabrication is generally involved the interaction between two types of flows: core flow and sheath flow. Core flow provides monomer, pre-polymer or polymer that would be solidified into fibers. Sheath flow could produce hydrodynamic focusing on the core flow to change the shape and size of the resulting fiber. Also, sheath flow might play a role in fiber solidification. The design of microchannel could be divided into three types. Concentric-flow geometry microchannel could produce hydrodynamic focusing easily but the shape of the fiber is generally limited to circular. Cross-flow geometry microchannel with built-in shaping elements not only could produce 3D hydrodynamic focusing but also has the capability to fabricate fibers with more complicated cross-sectional shapes. For fiber solidification, solvent extraction, chemical polymerization, and photopolymerization are three

main choices. To achieve fiber solidification via solvent extraction, the solvents of core solution and sheath solution should be specially selected. Polymerization of monomer or pre-polymer in the core fluid could also lead to solidification of fibers. Compared with chemical polymerization, photo-initiated polymerization has advantages of various kinds of available photo-curable monomers or pre-polymers, accurate shape-locking due to short reaction time, and also fewer materials gradients along the fiber [67].

2.4.4 Composite fiber fabrication using microfluidic method

As there are no strict requirements for the composition of the core fluid, an intriguing research area is to incorporate extra fillers or additives into core fluid to fabricate composite fibers [67]. Up to now, a few studies focusing microfluidic fabrication of composite fibers have been reported.

In order to produce satisfactory materials with mechanical reliability and viability for cell encapsulation, chitosan/alginate composite microfibers were fabricated using a cylindrical concentric-flow microfluidic device [78]. It was concluded that these is an approximately linear relationship between the diameter of the composite fibers and core flow speed with fixed sheath flow speed. The produced composite fibers showed better mechanical properties and encapsulation ability of HepG2 cell than alginate fibers. Hu et al. also successfully seeded human proximal tubule cells on the polysulfone composite fibers which were fabricated using a microfluidic method [79].

In addition to the easy fabrication of composite fibers because of the flexibility of the microfluidic technique, it is also achievable to incorporate cells directly into the fibers ascribed to the mild processing condition. Through introducing collagen/alginate/islets solution and

calcium chloride solution into a “Y” conjunction microchannel as core flow and sheath flow respectively, fabrication of islet-contained collage/alginate composite fibers was achieved [80]. It was demonstrated that the collage/alginate composite fiber could provide protection for islets from immune reactions during transplantation.

Methacrylated gelatin(GelMA)/alginate double-layer hollow composite fiber was fabricated using a cylindrical concentric-flow microchannel with three inlets [81]. Incorporation of GelMA increased the mechanical strength and decreased the swelling ratio of the fiber. Also, the microfluidic technique made it achievable to incorporate two kinds of cells into two layers of the fiber separately.

Shields et al. fabricated liquid crystal (LC) mesogen/acrylate composite fibers, which showed controllable cross-sectional shape and alignment of LC along the axial direction of the fiber [82]. With an aspect ratio larger than 1, the LC was oriented by the torque resulted from the non-uniform distribution of flow speed in the channel. The result showed promising potential to incorporate and align fillers with high aspect ratio in fibers through microfluidic method.

The interface between the fillers and matrix is one of the most important factors that determine the properties of composite materials. One viable approach to strength the interface is to chemically modify the surface of the fillers. Boyd et al. used ligands to functionalized the surface of gold nanoparticles which were then dispersed into the thiol-ene solution to be fabricated into composite fibers via the microfluidic method [83]. The fabricated composite fiber showed adjustable optical and mechanical properties through changing the content of gold nanoparticles incorporated.

In summary, owing to the flexibility of microfluidic fiber fabrication, various reinforcing or functional fillers could be incorporated into fibers through the microfluidic method. Also,

some sensitive biological materials could be embedded into the fibers due to the mild processing condition of microfluidic approach. Some studies have successfully fabricated composite fibers using the microfluidic method to increase the mechanical strength, endow fibers with optical properties and improve the cell encapsulation and proliferation. However, to the best of our knowledge, there has been no report for making electrically conductive composite fibers using a microfluidic platform.

2.5 References

[1] Y. Wang, X. Jing, Intrinsically conducting polymers for electromagnetic interference shielding, Polymers for advanced technologies 16(4) (2005) 344-351.

[2] K. Yoshino, M. Tabata, K. Kaneto, T. Ohsawa, Application and characteristics of conducting polymer as radiation shielding material, Japanese journal of applied physics 24(9A) (1985) L693.

[3] J. Pomposo, J. Rodrıguez, H. Grande, Polypyrrole-based conducting hot melt adhesives for EMI shielding applications, Synthetic Metals 104(2) (1999) 107-111.

[4] K. Desai, C. Sung, Electrospinning nanofibers of PANI/PMMA blends, MRS Proceedings, Cambridge Univ Press, 2002, p. D2. 7.

[5] D. Coltevieille, A. Le Méhauté, C. Challioui, P. Mirebeau, J.N. Demay, International Conference on Science and Technology of SyntheticIndustrial applications of polyaniline, Synthetic Metals 101(1) (1999) 703-704.

[6] S. Li, Y. Cao, Z. Xue, Soluble polyaniline, Synthetic Metals 20(2) (1987) 141-149.

[7] A. Andreatta, Y. Cao, J.C. Chiang, A.J. Heeger, P. Smith, Electrically-conductive fibers of polyaniline spun from solutions in concentrated sulfuric acid, Synthetic Metals 26(4) (1988) 383-389.

[8] A. Andreatta, S. Tokito, P. Smith, A.J. Heeger, High Performance Fibers of Conducting Polymers, Molecular Crystals and Liquid Crystals Incorporating Nonlinear Optics 189(1) (1990) 169-182.

[9] S.J. Pomfret, P.N. Adams, N.P. Comfort, A.P. Monkman, Electrical and mechanical properties of polyaniline fibres produced by a one-step wet spinning process, Polymer 41(6) (2000) 2265-2269.

[10] J.H. Yu, S.V. Fridrikh, G.C. Rutledge, The role of elasticity in the formation of electrospun fibers, Polymer 47(13) (2006) 4789-4797.

[11] Y. Zhang, G.C. Rutledge, Electrical Conductivity of Electrospun Polyaniline and Polyaniline-Blend Fibers and Mats, Macromolecules 45(10) (2012) 4238-4246.

[12] L. Nyholm, G. Nyström, A. Mihranyan, M. Strømme, Toward Flexible Polymer and Paper-Based Energy Storage Devices, Advanced Materials 23(33) (2011) 3751-3769.

[13] H.K. Kim, M.S. Kim, S.Y. Chun, Y.H. Park, B.S. Jeon, J.Y. Lee, Y.K. Hong, J. Joo, S.H. Kim, Characteristics of electrically conducting polymer-coated textiles, Mol. Cryst. Liq. Cryst. 405(1) (2003) 161-169.

[14] Y. Ding, M.A. Invernale, G.A. Sotzing, Conductivity Trends of PEDOT-PSS Impregnated Fabric and the Effect of Conductivity on Electrochromic Textile, ACS Applied Materials & Interfaces 2(6) (2010) 1588-1593.

[15] B. Kim, V. Koncar, E. Devaux, C. Dufour, P. Viallier, Electrical and morphological properties of PP and PET conductive polymer fibers, Synthetic Metals 146(2) (2004) 167-174.

[16] B. Zhang, T. Xue, J. Meng, H. Li, Study on property of PANI/PET composite conductive fabric, The Journal of The Textile Institute 106(3) (2015) 253-259.

[17] M.S. Kim, H.K. Kim, S.W. Byun, S.H. Jeong, Y.K. Hong, J.S. Joo, K.T. Song, J.K. Kim, C.J. Lee, J.Y. Lee, PET fabric/polypyrrole composite with high electrical conductivity for EMI shielding, Synthetic Metals 126(2–3) (2002) 233-239.

[18] D. Knittel, E. Schollmeyer, Electrically high-conductive textiles, Synthetic Metals 159(14) (2009) 1433-1437.

[19] T. Bashir, L. Fast, M. Skrifvars, N.-K. Persson, Electrical resistance measurement methods and electrical characterization of poly(3,4-ethylenedioxythiophene)-coated conductive fibers, Journal of Applied Polymer Science 124(4) (2012) 2954-2961.
[20] B.S. Shim, W. Chen, C. Doty, C. Xu, N.A. Kotov, Smart Electronic Yarns and Wearable Fabrics for Human Biomonitoring made by Carbon Nanotube Coating with Polyelectrolytes, Nano Letters 8(12) (2008) 4151-4157.

[21] P. Xue, K.H. Park, X.M. Tao, W. Chen, X.Y. Cheng, Electrically conductive yarns based on PVA/carbon nanotubes, Composite Structures 78(2) (2007) 271-277.

[22] C. Robert, J.F. Feller, M. Castro, Sensing Skin for Strain Monitoring Made of PC–CNT Conductive Polymer Nanocomposite Sprayed Layer by Layer, ACS Applied Materials & Interfaces 4(7) (2012) 3508-3516.

[23] N. Bhardwaj, S.C. Kundu, Electrospinning: A fascinating fiber fabrication technique, Biotechnology Advances 28(3) (2010) 325-347.

[24] T.J. Sill, H.A. von Recum, Electrospinning: Applications in drug delivery and tissue engineering, Biomaterials 29(13) (2008) 1989-2006.

[25] Z.-M. Huang, Y.Z. Zhang, M. Kotaki, S. Ramakrishna, A review on polymer nanofibers by electrospinning and their applications in nanocomposites, Composites Science and Technology 63(15) (2003) 2223-2253.

[26] A. Baji, Y.-W. Mai, S.-C. Wong, M. Abtahi, P. Chen, Electrospinning of polymer nanofibers: Effects on oriented morphology, structures and tensile properties, Composites Science and Technology 70(5) (2010) 703-718.

[27] J.S. Jeong, J.S. Moon, S.Y. Jeon, J.H. Park, P.S. Alegaonkar, J.B. Yoo, Mechanical properties of electrospun PVA/MWNTs composite nanofibers, Thin Solid Films 515(12) (2007) 5136-5141.

[28] M.J. O'Connell, P. Boul, L.M. Ericson, C. Huffman, Y. Wang, E. Haroz, C. Kuper, J. Tour, K.D. Ausman, R.E. Smalley, Reversible water-solubilization of single-walled carbon nanotubes by polymer wrapping, Chemical physics letters 342(3) (2001) 265-271.

[29] H. Hou, J.J. Ge, J. Zeng, Q. Li, D.H. Reneker, A. Greiner, S.Z.D. Cheng, Electrospun Polyacrylonitrile Nanofibers Containing a High Concentration of Well-Aligned Multiwall Carbon Nanotubes, Chemistry of Materials 17(5) (2005) 967-973.

[30] W. Salalha, Y. Dror, R.L. Khalfin, Y. Cohen, A.L. Yarin, E. Zussman, Single-Walled Carbon Nanotubes Embedded in Oriented Polymeric Nanofibers by Electrospinning, Langmuir 20(22) (2004) 9852-9855.

[31] S. Kedem, J. Schmidt, Y. Paz, Y. Cohen, Composite Polymer Nanofibers with Carbon Nanotubes and Titanium Dioxide Particles, Langmuir 21(12) (2005) 5600-5604.
[32] B. Sundaray, V. Subramanian, T.S. Natarajan, K. Krishnamurthy, Electrical conductivity of a single electrospun fiber of poly(methyl methacrylate) and multiwalled carbon nanotube nanocomposite, Applied Physics Letters 88(14) (2006) 143114.

[33] L. Ghasemi-Mobarakeh, M.P. Prabhakaran, M. Morshed, M.H. Nasr-Esfahani, S. Ramakrishna, Electrical stimulation of nerve cells using conductive nanofibrous scaffolds for nerve tissue engineering, Tissue Engineering Part A 15(11) (2009) 3605-3619.

[34] T.H. Lim, S.H. Lee, S.Y. Yeo, Highly conductive polymer/metal/carbon nanotube composite fiber prepared by the melt-spinning process, Textile Research Journal (2016).

[35] R. Haggenmueller, H.H. Gommans, A.G. Rinzler, J.E. Fischer, K.I. Winey, Aligned single-wall carbon nanotubes in composites by melt processing methods, Chemical Physics Letters 330(3–4) (2000) 219-225.

[36] T.D. Fornes, J.W. Baur, Y. Sabba, E.L. Thomas, Morphology and properties of melt-spun polycarbonate fibers containing single- and multi-wall carbon nanotubes, Polymer 47(5) (2006) 1704-1714.

[37] Y. Zhu, Y. Zhao, X. Zhang, L. Wang, X. Wang, J. Zhang, P. Han, J. Qiao, Metal filaments/nano-filler filled hybrid polymer fibers with improved conductive performance, Materials Letters 173 (2016) 26-30.

[38] E.A. Morris, M.C. Weisenberger, Solution Spinning of PAN-Based Polymers for Carbon Fiber Precursors, Polymer Precursor-Derived Carbon, American Chemical Society2014, pp. 189-213.

[39] S. Seyedin, J.M. Razal, P.C. Innis, A. Jeiranikhameneh, S. Beirne, G.G. Wallace, Knitted Strain Sensor Textiles of Highly Conductive All-Polymeric Fibers, ACS Applied Materials & Interfaces 7(38) (2015) 21150-21158.

[40] R. Ma, J. Lee, D. Choi, H. Moon, S. Baik, Knitted Fabrics Made from Highly Conductive Stretchable Fibers, Nano Letters 14(4) (2014) 1944-1951.

[41] T. Sekitani, H. Nakajima, H. Maeda, T. Fukushima, T. Aida, K. Hata, T. Someya, Stretchable active-matrix organic light-emitting diode display using printable elastic conductors, Nature materials 8(6) (2009) 494-499.

[42] A.-T. Chien, P.V. Gulgunje, H.G. Chae, A.S. Joshi, J. Moon, B. Feng, G.P. Peterson, S. Kumar, Functional polymer–polymer/carbon nanotube bi-component fibers, Polymer 54(22) (2013) 6210-6217.

[43] H. Deng, T. Skipa, E. Bilotti, R. Zhang, D. Lellinger, L. Mezzo, Q. Fu, I. Alig, T. Peijs, Preparation of High-Performance Conductive Polymer Fibers through Morphological Control of Networks Formed by Nanofillers, Advanced Functional Materials 20(9) (2010) 1424-1432.
[44] E.K. Sackmann, A.L. Fulton, D.J. Beebe, The present and future role of microfluidics in biomedical research, Nature 507(7491) (2014) 181-189.

[45] S.H. Lee, A.J. Heinz, S. Shin, Y.-G. Jung, S.-E. Choi, W. Park, J.-H. Roe, S. Kwon, Capillary based patterning of cellular communities in laterally open channels, Analytical chemistry 82(7) (2010) 2900-2906.

[46] D.J. Beebe, G.A. Mensing, G.M. Walker, Physics and applications of microfluidics in biology, Annual review of biomedical engineering 4(1) (2002) 261-286.

[47] D. Sinton, Energy: the microfluidic frontier, Lab on a Chip 14(17) (2014) 3127-3134.

[48] S.M. Mitrovski, L.C. Elliott, R.G. Nuzzo, Microfluidic devices for energy conversion: Planar integration and performance of a passive, fully immersed H2-O2 fuel cell, Langmuir 20(17) (2004) 6974-6976.

[49] F. Sharifi, S. Ghobadian, F.R. Cavalcanti, N. Hashemi, Paper-based devices for energy applications, Renewable and Sustainable Energy Reviews 52 (2015) 1453-1472.

[50] F. Sharifi, D. Kurteshi, N. Hashemi, Designing highly structured polycaprolactone fibers using microfluidics, Journal of the Mechanical Behavior of Biomedical Materials 61 (2016) 530-540.

[51] A. Dector, R.A. Escalona-Villalpando, D. Dector, V. Vallejo-Becerra, A.U. Chávez-Ramírez, L.G. Arriaga, J. Ledesma-García, Perspective use of direct human blood as an energy source in air-breathing hybrid microfluidic fuel cells, Journal of Power Sources 288 (2015) 70-75.

[52] H.L. Harvinder Lal, S.S.Sehgal, Evaluation of micromachining processes for fabrication of micro-channels, International Journal of Latest Trends in Engineering and Technology (IJLTET), 2012, pp. 105-108.

[53] S. Ashman, S.G. Kandlikar, A review of manufacturing processes for microchannel heat exchanger fabrication, ASME 4th International Conference on Nanochannels, Microchannels, and Minichannels, American Society of Mechanical Engineers, 2006, pp. 855-860.

[54] C.P. Beetz, R. Boerstler, J. Steinbeck, B. Lemieux, D.R. Winn, Silicon-micromachined microchannel plates, Nuclear Instruments and Methods in Physics Research Section A: Accelerators, Spectrometers, Detectors and Associated Equipment 442(1–3) (2000) 443-451.

[55] K.B. Lee, L. Lin, Surface micromachined glass and polysilicon microchannels using MUMPs for BioMEMS applications, Sensors and Actuators A: Physical 111(1) (2004) 44-50.

[56] S.-J. Qin, W.J. Li, Micromachining of complex channel systems in 3D quartz substrates using Q-switched Nd:YAG laser, Applied Physics A 74(6) (2002) 773-777.
[57] I. Papautsky, J. Brazzle, H. Swerdlow, A.B. Frazier, A low-temperature IC-compatible process for fabricating surface-micromachined metallic microchannels, Journal of microelectromechanical systems 7(2) (1998) 267-273.

[58] J. Xu, L. Locascio, M. Gaitan, C.S. Lee, Room-Temperature Imprinting Method for Plastic Microchannel Fabrication, Analytical Chemistry 72(8) (2000) 1930-1933.

[59] G.T.A. Kovacs, N.I. Maluf, K.E. Petersen, Bulk micromachining of silicon, Proceedings of the IEEE 86(8) (1998) 1536-1551.

[60] J.M. Bustillo, R.T. Howe, R.S. Muller, Surface micromachining for microelectromechanical systems, Proceedings of the IEEE 86(8) (1998) 1552-1574.

[61] K.B. Lee, L. Lin, Surface micromachined glass and polysilicon microchannels using MUMPs, Micro Electro Mechanical Systems, 2003. MEMS-03 Kyoto. IEEE The Sixteenth Annual International Conference on, IEEE, 2003, pp. 578-581.

[62] P. Kim, K.W. Kwon, M.C. Park, S.H. Lee, S.M. Kim, K.Y. Suh, Soft lithography for microfluidics: a review, (2008).

[63] J. O'Connor, J. Punch, N. Jeffers, J. Stafford, A dimensional comparison between embedded 3D-printed and silicon microchannels, Journal of Physics: Conference Series, IOP Publishing, 2014, p. 012009.

[64] P.J. Goodrich, F. Sharifi, N. Hashemi, Rapid prototyping of microchannels with surface patterns for fabrication of polymer fibers, RSC Advances 5(87) (2015) 71203-71209.

[65] M.A. Roberts, J.S. Rossier, P. Bercier, H. Girault, UV Laser Machined Polymer Substrates for the Development of Microdiagnostic Systems, Analytical Chemistry 69(11) (1997) 2035-2042.

[66] C. Khoury, G.A. Mensing, D.J. Beebe, Ultra rapid prototyping of microfluidic systems using liquid phase photopolymerization, Lab on a Chip 2(1) (2002) 50-55.

[67] M.A. Daniele, D.A. Boyd, A.A. Adams, F.S. Ligler, Microfluidic Strategies for Design and Assembly of Microfibers and Nanofibers with Tissue Engineering and Regenerative Medicine Applications, Advanced Healthcare Materials 4(1) (2015) 11-28.

[68] Z. Bai, J.M. Mendoza Reyes, R. Montazami, N. Hashemi, On-chip development of hydrogel microfibers from round to square/ribbon shape, Journal of Materials Chemistry A 2(14) (2014) 4878-4884.

[69] D.A. Boyd, A.A. Adams, M.A. Daniele, F.S. Ligler, Microfluidic Fabrication of Polymeric and Biohybrid Fibers with Predesigned Size and Shape, Journal of Visualized Experiments : JoVE (83) (2014) 50958.

[70] E. Kang, Y.Y. Choi, S.-K. Chae, J.-H. Moon, J.-Y. Chang, S.-H. Lee, Microfluidic Spinning of Flat Alginate Fibers with Grooves for Cell-Aligning Scaffolds, Advanced Materials 24(31) (2012) 4271-4277.

[71] C.M. Hwang, A. Khademhosseini, Y. Park, K. Sun, S.-H. Lee, Microfluidic Chip-Based Fabrication of PLGA Microfiber Scaffolds for Tissue Engineering, Langmuir 24(13) (2008) 6845-6851.

[72] J. Cheng, D. Park, Y. Jun, J. Lee, J. Hyun, S.-H. Lee, Biomimetic spinning of silk fibers and in situ cell encapsulation, Lab on a Chip (2016).

[73] A. Duboin, R. Middleton, F. Malloggi, F. Monti, P. Tabeling, Cusps, spouts and microfiber synthesis with microfluidics, Soft Matter 9(11) (2013) 3041-3049.

[74] J.K. Nunes, C.-Y. Wu, H. Amini, K. Owsley, D. Di Carlo, H.A. Stone, Fabricating Shaped Microfibers with Inertial Microfluidics, Advanced Materials 26(22) (2014) 3712-3717.

[75] A.L. Thangawng, P.B. Howell Jr, J.J. Richards, J.S. Erickson, F.S. Ligler, A simple sheath-flow microfluidic device for micro/nanomanufacturing: fabrication of hydrodynamically shaped polymer fibers, Lab on a Chip 9(21) (2009) 3126-3130.

[76] F. Sharifi, Z. Bai, R. Montazami, N. Hashemi, Mechanical and physical properties of poly(vinyl alcohol) microfibers fabricated by a microfluidic approach, RSC Advances 6(60) (2016) 55343-55353.

[77] X. Shi, S. Ostrovidov, Y. Zhao, X. Liang, M. Kasuya, K. Kurihara, K. Nakajima, H. Bae, H. Wu, A. Khademhosseini, Microfluidic Spinning of Cell-Responsive Grooved Microfibers, Advanced Functional Materials 25(15) (2015) 2250-2259.

[78] B.R. Lee, K.H. Lee, E. Kang, D.-S. Kim, S.-H. Lee, Microfluidic wet spinning of chitosan-alginate microfibers and encapsulation of HepG2 cells in fibers, Biomicrofluidics 5(2) (2011) 022208.

[79] M. Hu, R. Deng, K.M. Schumacher, M. Kurisawa, H. Ye, K. Purnamawati, J.Y. Ying, Hydrodynamic spinning of hydrogel fibers, Biomaterials 31(5) (2010) 863-869.

[80] Y. Jun, M.J. Kim, Y.H. Hwang, E.A. Jeon, A.R. Kang, S.-H. Lee, D.Y. Lee, Microfluidics-generated pancreatic islet microfibers for enhanced immunoprotection, Biomaterials 34(33) (2013) 8122-8130.

[81] Y. Zuo, X. He, Y. Yang, D. Wei, J. Sun, M. Zhong, R. Xie, H. Fan, X. Zhang, Microfluidic-based generation of functional microfibers for biomimetic complex tissue construction, Acta Biomaterialia 38 (2016) 153-162.
[82] A.R. Shields, C.M. Spillmann, J. Naciri, P.B. Howell, A.L. Thangawng, F.S. Ligler, Hydrodynamically directed multiscale assembly of shaped polymer fibers, Soft Matter 8(24) (2012) 6656-6660.

[83] D.A. Boyd, J. Naciri, J. Fontana, D.B. Pacardo, A.R. Shields, J. Verbarg, C.M. Spillmann, F.S. Ligler, Facile Fabrication of Color Tunable Film and Fiber Nanocomposites via Thiol Click Chemistry, Macromolecules 47(2) (2014) 695-704.

CHAPTER 3

FABRICATION OF MOLDS AND MICROCHANNEL

In this thesis work, the microfluidic channel was made by polydimethylsiloxane (PDMS) through molding replication. To perform molding replication of PDMS, two master molds were made by micromachining of poly(methyl methacrylate) (PMMA) substrates using computer numerical control (CNC) micro milling machine (Mini-Mill-GX, Minitech Machinery Corp).

The design of the microchannel created by Solidworks is shown in **Figure 1**. The microchannel consists of three inlets and one outlet. Core fluid was introduced into the inlet in the middle. Sheath fluid was introduced into the two inlets on both sides. Four chevron-shaped grooves were built on the ceiling and bottom of the channel.

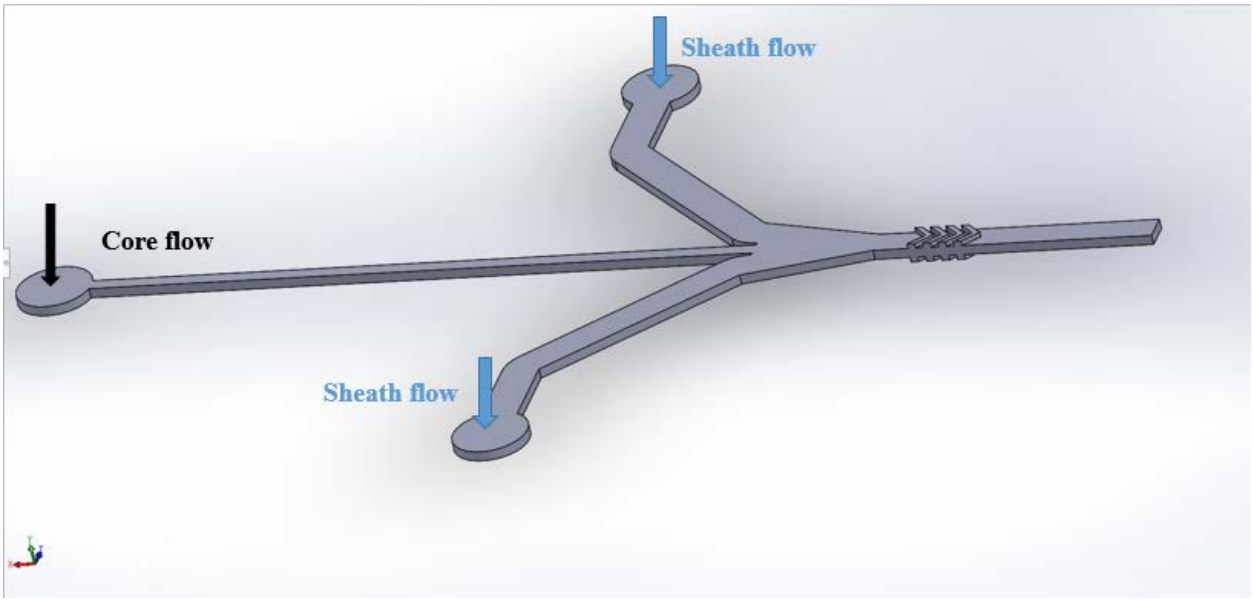

Figure 1. *Design of Microchannel for Microfluidic Fiber Fabrication*

Figure 2 shows the dimension of the microchannel. The height and width of the channel are 200 µm and 600 µm respectively. The 90˚ chevron grooves are 100 µm in height and 155 µm in width. The distance between the grooves is 155 µm.

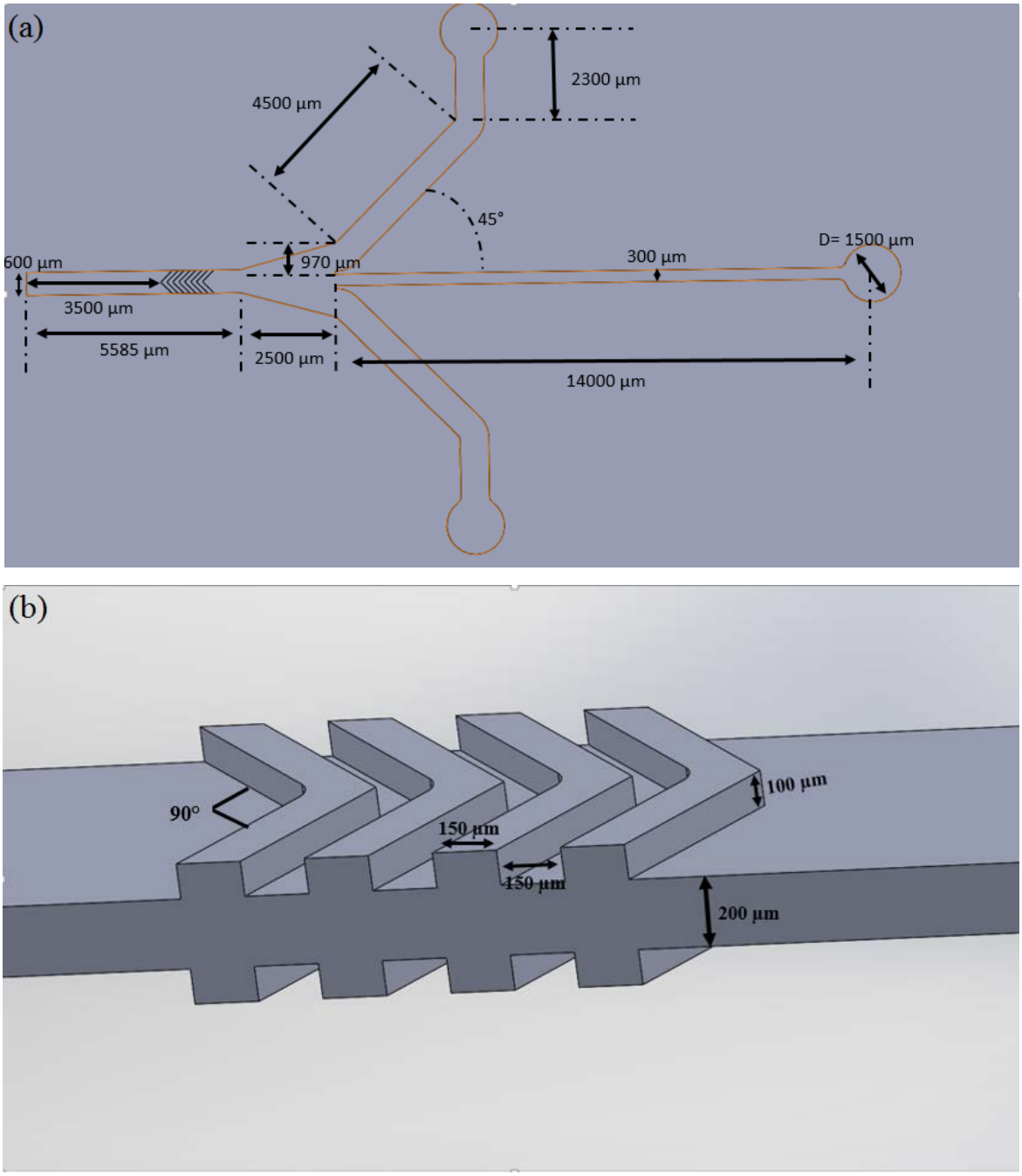

Figure 2. *The dimension of (a) microfluidic channel and (b) chevron grooves*

3.1 Fabrication of Master Molds for Microchannel

The master molds with the negative image of the design are shown in **Figure 3**.

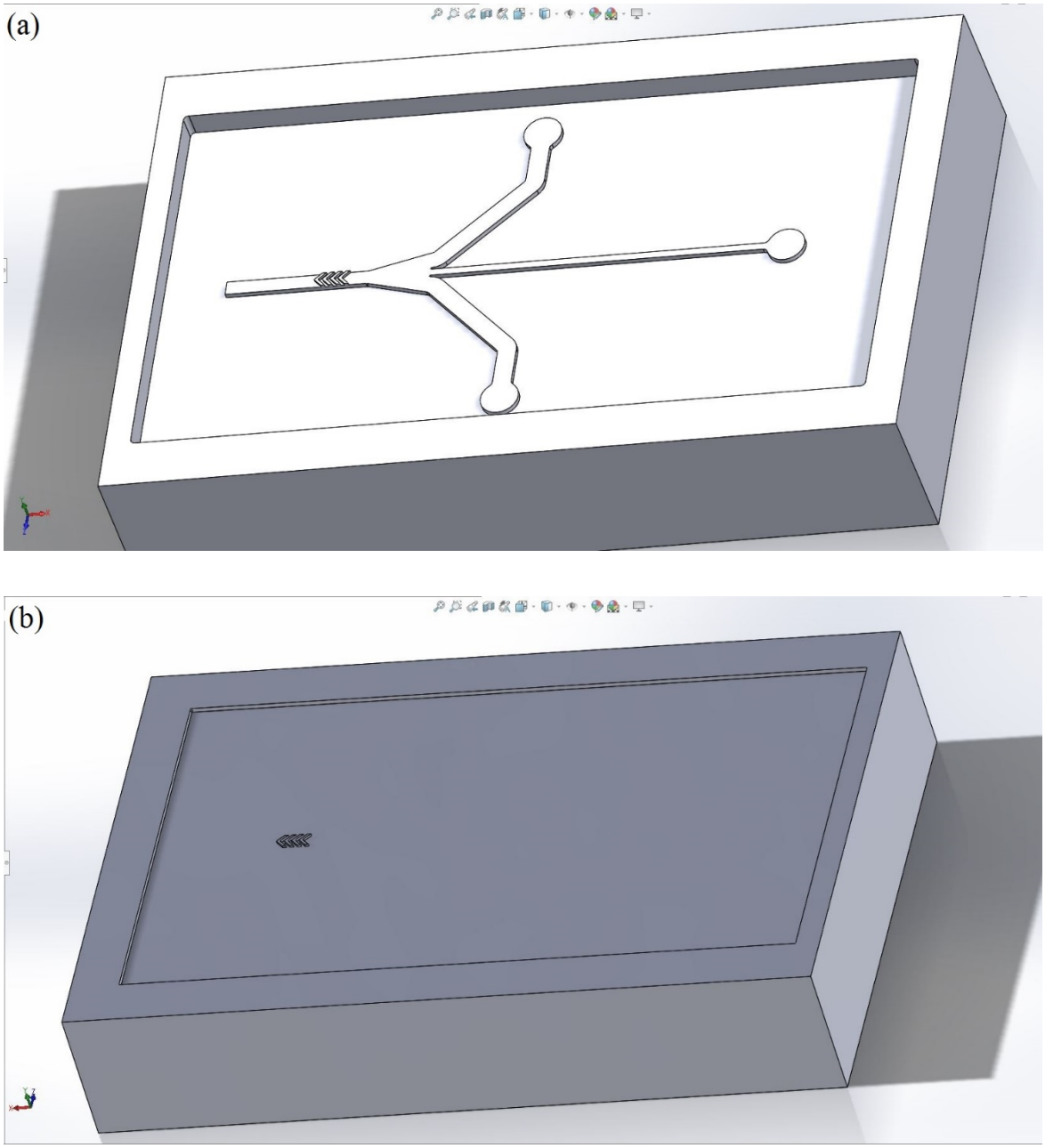

Figure 3. *The dimension of (a) microfluidic channel and (b) chevron grooves*

The master molds were fabricated by milling of PMMA substrates using a CNC micro milling machine. An end mill (1#) with the cutter diameter of 0.015 inches and 0.045 inches in length of cut was used to mill the main channel. An end mill (2#) with the cutter diameter of 0.003 inches and 0.009 inches in length of cut was used to mill the chevron-shaped grooves. The milling parameters are listed in **Table 1**. As low feed rate and high spindle rotational speed could result in smooth surfaces [1], the spindle speed was set at 27000 rpm. The feed rates for tool 1# and 2# were set as 15 mm/min and 2.5 mm/min respectively. There are two kinds of ways to mill materials, conventional milling and climb milling. As opposed to conventional milling, the tool rotates against the feed direction for climb milling. In general, climb milling would produce less stress on the milling tools and result in a smoother surface than conventional milling [2]. So climb milling was selected.

Table 1. *Milling parameter of two types of end mills*

Tool #	1#	2#
Diameter/inch	0.015	0.003
Length of cut/inch	0.045	0.009
Feed rate/mm·min^{-1}	15	2.5
Spindle speed/rpm	27000	27000
Plunge rate/mm·min^{-1}	1.0	0.2
Machining direction	Climb	Climb
Cutting method	Parallel spiral	Parallel spiral
Stepover percentage	20%	20%

The G-code for CNC-milling was produced by using Mastercam 2015. The beginning and end of the G-code were shown in **Table 2**.

Table 2. *The beginning of G-code for CNC-milling*

Tool 1#	Tool 2#
% (T1 | 0.381 FLAT ENDMILL | H1) G21 G0 G17 G40 G49 G80 G90 G0 Z5. G0 G90 G54 X11.963 Y-11.944 S27000 M3 G0 Z1. G1 Z0. F1. Y-15.999 F15. … … G0 Z10. M5 G0 X0. Y0. M30 %	% (T2 | 0.0762 FLAT ENDMILL | H2) G21 G0 G17 G40 G49 G80 G90 G0 Z5. G0 G90 G54 X11.992 Y-21.653 S27000 M3 G0 Z1. G1 Z-.09 F.2 X12. Y-21.661 F2.5 … … G0 Z10. M5 G0 X0. Y0. M30 %

G21 sets the unit of coordinate as mm. G0 means moving the tool straightly at high speed. The milling plane is set as the X-Y plane by G17. G40 and G49 could cancel the tool cutter and length compensation respectively. G80 cancels the canned cycle. G90 means the G-

code is based on an absolute X-Y-Z coordinate system. M5 is used to stop the rotation of the spindle. M30 means the end of the program. The code begins with % and ends with %.

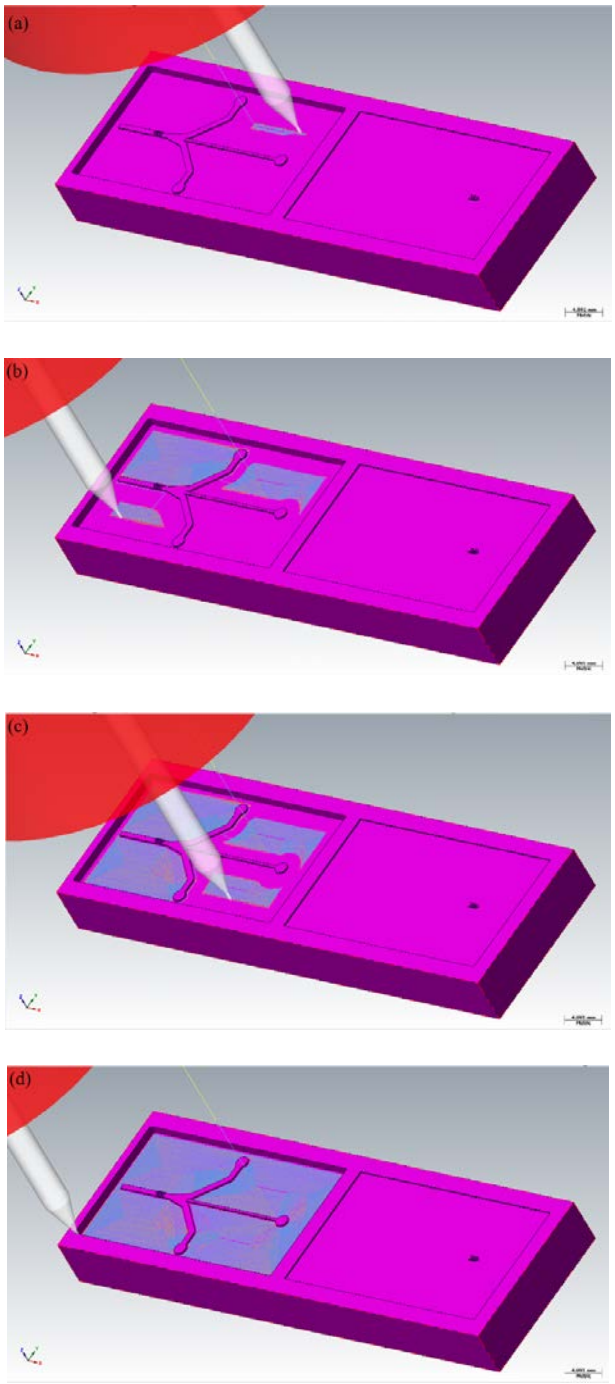

Figure 4. *Milling procedures of the main channel*

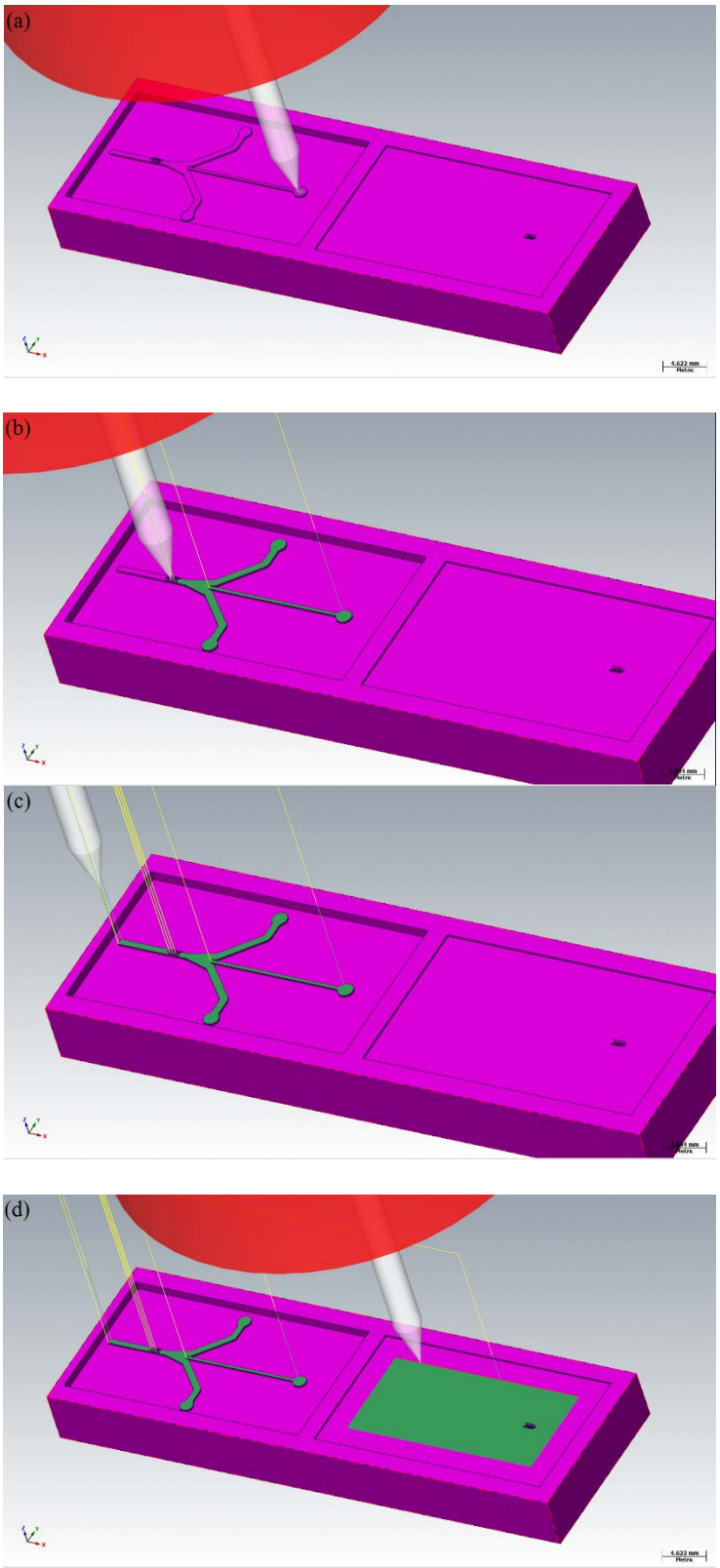

Figure 5. *Milling procedures of chevron-shaped grooves*

The milling procedures of the main channel and chevron-shaped grooves are shown in **Figure 4** and **5** respectively.

In order to further smoothen surfaces of the as-machined PMMA master molds, exposure of chloroform vapor was performed [3]. As shown in **Figure 6**, the sealed chloroform vapor environment was produced by three petri dishes and water bath. The PMMA master molds were exposed to chloroform vapor for 40 seconds at room temperature. As the surfaces of PMMA master molds could be softened at a similar rate by the chloroform vapor [3], the surface of PMMA tended to be smooth due to surface tension.

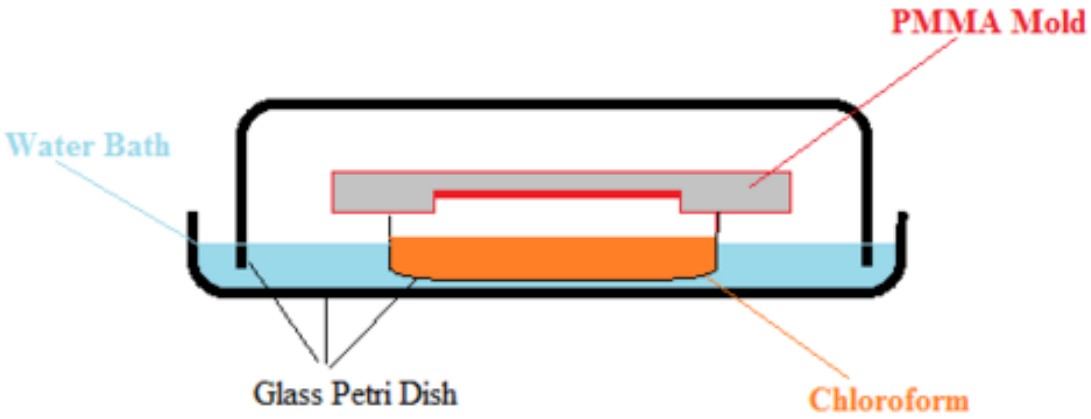

Figure 6. *Illustration of PMMA master mold exposed to chloroform vapor*

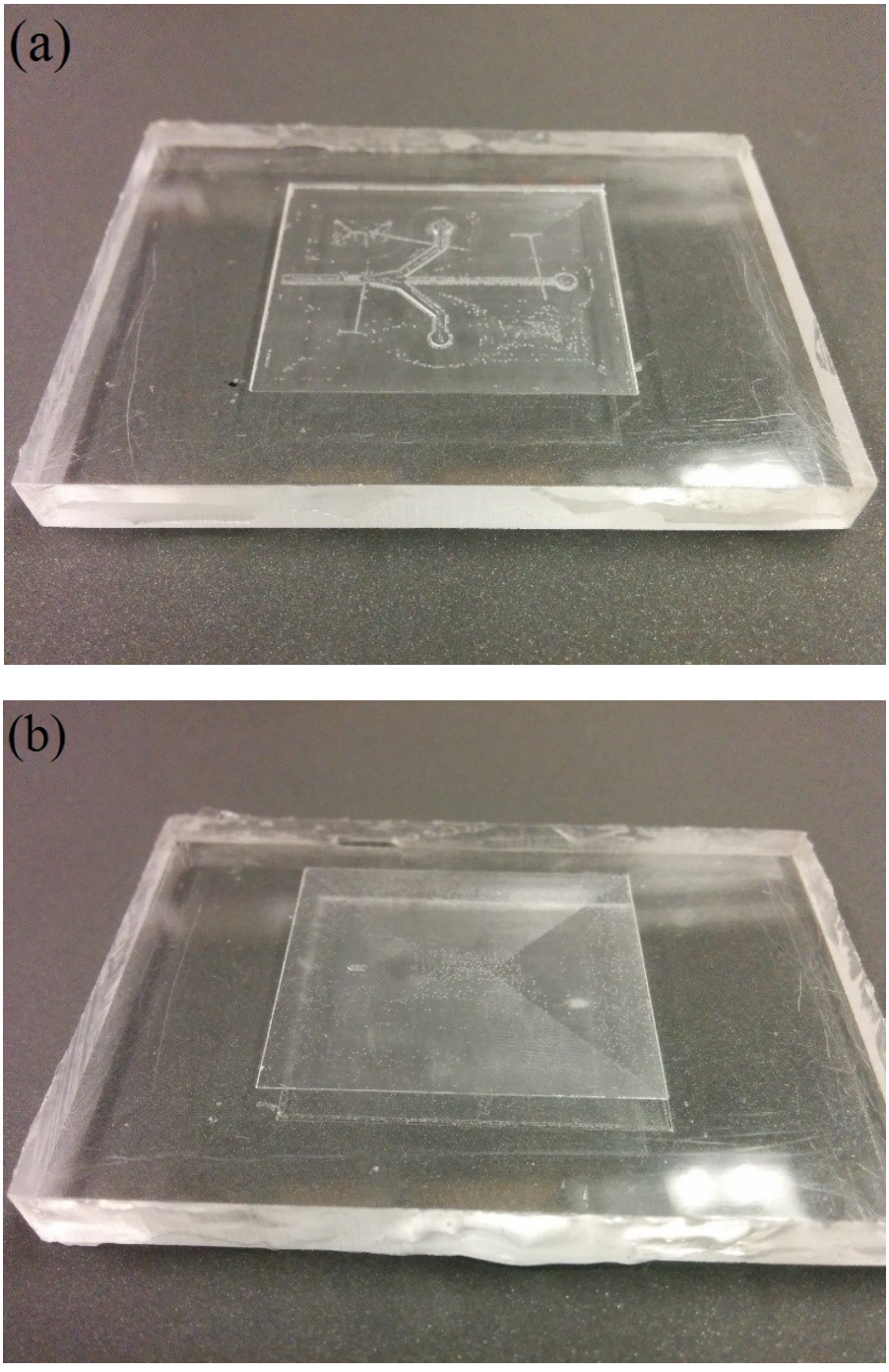

Figure 7. *PMMA master molds*

The completed master molds ready for soft-lithography are shown in **Figure 7**.

3.2 Fabrication of Microchannel by Molding Replication

The microfluidic channel for fiber fabrication was prepared by molding replication based on the as-fabricated PMMA master molds. In detail, Sylgard 184 Elastomer Base and Curing Agent were mixed with a w/w ratio of 10:1, and then poured over two PMMA molds made by a CNC micro milling machine (Mini-Mill-GX, Minitech Machinery Corp). After curing at 85 °C for 25 minutes, two half layers of the microchannel were peeled off from the PMMA master molds. The top half layer of the microchannel was bonded with a PDMS substrate via plasma treatment. After waiting for 24 hours, three holes were punched as inlets. Then the microchannel was assembled by bonding the top half layer with another half layer via plasma treatment. After waiting for 24 hours, plastic tubing was inserted into the three inlets and fixed by epoxy glue. The integrated microchannel ready for microfluidic fiber fabrication was shown in **Figure 8**.

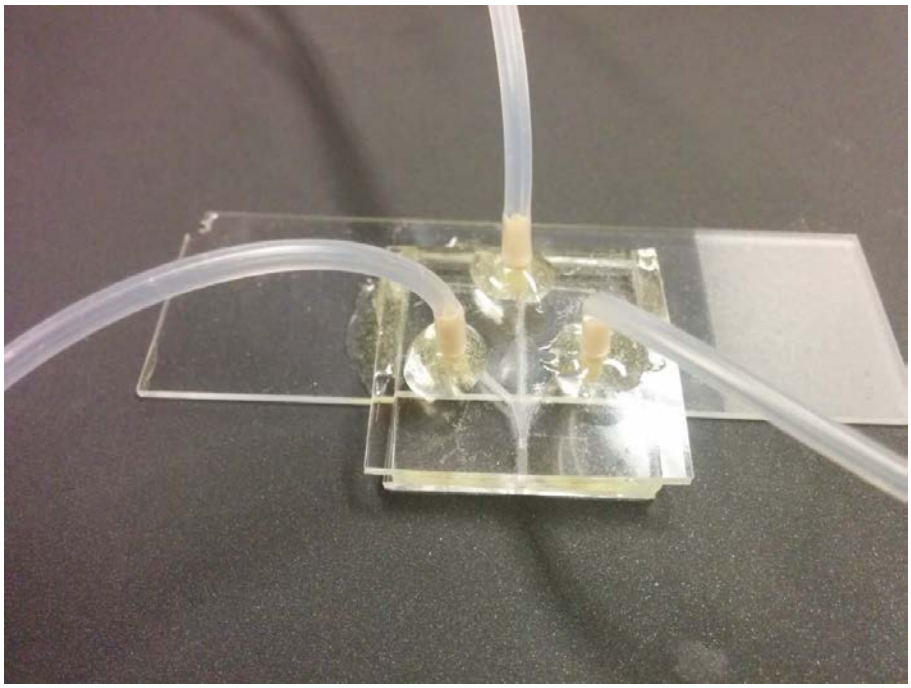

Figure 8. *Integrated microchannel ready for fiber fabrication*

3.3 References

[1] J.-H. Wang, L. Cheng, C.-H. Wang, W.-S. Ling, S.-W. Wang, G.-B. Lee, Biosensors and Bioelectronics, 41 (2013) 484-491.

[2] W. Kline, R. DeVor, I. Shareef, Journal of Engineering for Industry, 104 (1982) 272-278.

[3] I. Ogilvie, V.J. Sieben, C. Floquet, R. Zmijan, M. Mowlem, H. Morgan, 14 th International Conference on Miniaturized System for Chemistry and Life Sciences, 2010, pp. 1244-1246.

CHAPTER 4
MICROFLUIDIC FABRICATION OF ELECTRICALLY CONDUCTIVE CNF/PCL COMPOSITE FIBER

In this section, carbon nanofiber (CNF) and Polycaprolactone (PCL), which is a biocompatible and biodegradable polymer, were selected as the electrically conductive filler and the polymer matrix, respectively. Electrically conductive CNF/PCL composite fibers were fabricated using a microfluidic approach for the first time.

4.1 Experimental Section

4.1.1 Materials

Sylgard 184 Elastomer Base and Curing Agent were obtained from Dow Croning Corporation (Midland, MI). Polycaprolactone (PCL) (M_n=80,000), carbon nanofiber (CNF) (D×L=100 nm × 20-200μm), and polyethylene glycol (PEG) (Mn=20,000) were purchased from Sigma Aldrich (St. Louis, MO). 2,2,2-trifluoroethanol (TFE) was obtained from Oakwood Chemical (West Columbia, SC).

4.1.2 Preparation of Core and Sheath Solutions

Core fluid: In order to achieve good dispersion of CNFs in PCL solution, CNFs were first dispersed into the PCL solution of low concentration, which was mixed with the PCL solution of high concentration. CNFs were dispersed into a PCL solution of low concentration at 1.25% (0.05g PCL dissolved in 4 mL TFE). The concentration of the CNFs are with respect to the weight of PCL (i.e. 3 wt.% of CNF means that weight ratio of CNFs and PCL is 3:100). After transferring the CNFs suspension, 2 mL of TFE was used to rinse the container in order to capture the residual material. The CNF suspension was magnetically stirred for 30 minutes then

ultrasonicated for another 30 minutes at room temperature. After preparing the CNFs suspension, it was poured into a PCL/TFE solution of high concentration at 36.25% (1.45g PCL dissolved in 4 mL TFE) which was thoroughly mixed at 65 ℃ for 4 hours then further mixed at room temperature throughout the rest of the night with constant magnetic stirring. Finally, the suspension was ultrasonicated at 65℃ for 90 minutes. The CNF suspension was cooled to room temperature during magnetic stirring. Before the fiber fabrication process, the solution was rested for at least 15 minutes.

Sheath fluid: 15% g/mL PEG was dissolved into the mixture of DI water and ethanol with a volume ratio of 1:1.

Bath: The mixture of DI water and ethanol at a volume ratio of 1:1 was used as bath for collecting fibers.

The core fluid and sheath fluid were loaded into 3 mL and 60 mL plastic syringes (BD Biosciences) and pumped into the microchannel using a double syringe pump (Cole-Parmer, Veron Hillss, IL). The core and sheath flow rate ratios were set as 50:10 µL/min, 40:10 µL/min, 30:10 µL/min, and 20 µL/min.

4.1.3 Microfluidic Fiber Fabrication

The laminar flow regime was used in this experiment. Therefore, the diffusion occurred only at the fluid/fluid interface. **Figure 9** shows a schematic of the microfluidic fiber fabrication. As the core and sheath fluids entered the microchannel, the sheath flow exerted lateral hydrodynamic shear force on the core flow at the junction of the three inlets [1]. As shown in **Figure 9**, the microchannel has four chevron grooves. Due to the hydrodynamic resistance being inversely dependent on the flow rate and the sheath flow rate having higher values compared to

the core flow rate, the sheath fluid filled the chevron grooves at the top and bottom of the microchannel. As a result, the sheath fluid exerted vertical force on the core fluid as well as lateral force, which resulted in wrapping around the core fluid, and focusing it at the center of the channel [2]. In this process, the shear force plays a significant role in changing the shape of the resulting fiber as well as aligning the CNFs and polymer chain along the flow direction. We used the phase inversion solidification strategy in this process, which means that the molecules of the TFE were replaced by the molecules of the sheath fluid (water and ethanol) at the core/sheath interface. Because PCL is not soluble in the sheath fluid, it was solidified as a fiber at the outlet of the channel.

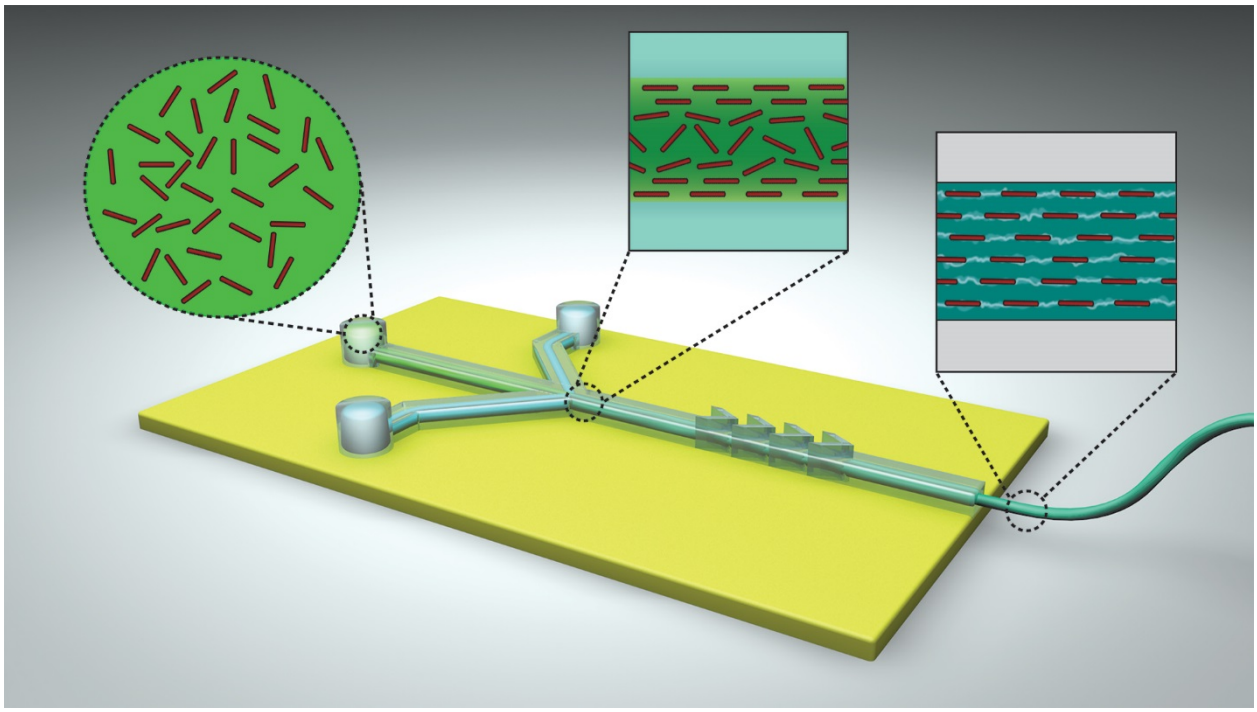

Figure 9. *Schematic illustration of microfluidic fiber fabrication*

4.1.4 Characterization

The morphology and cross-sectional properties of the prepared fibers were investigated using Scanning Electron Microscopy (NeoScopo, JCM-6000 Benchtop SEM) and the Dino Lite Microscope.

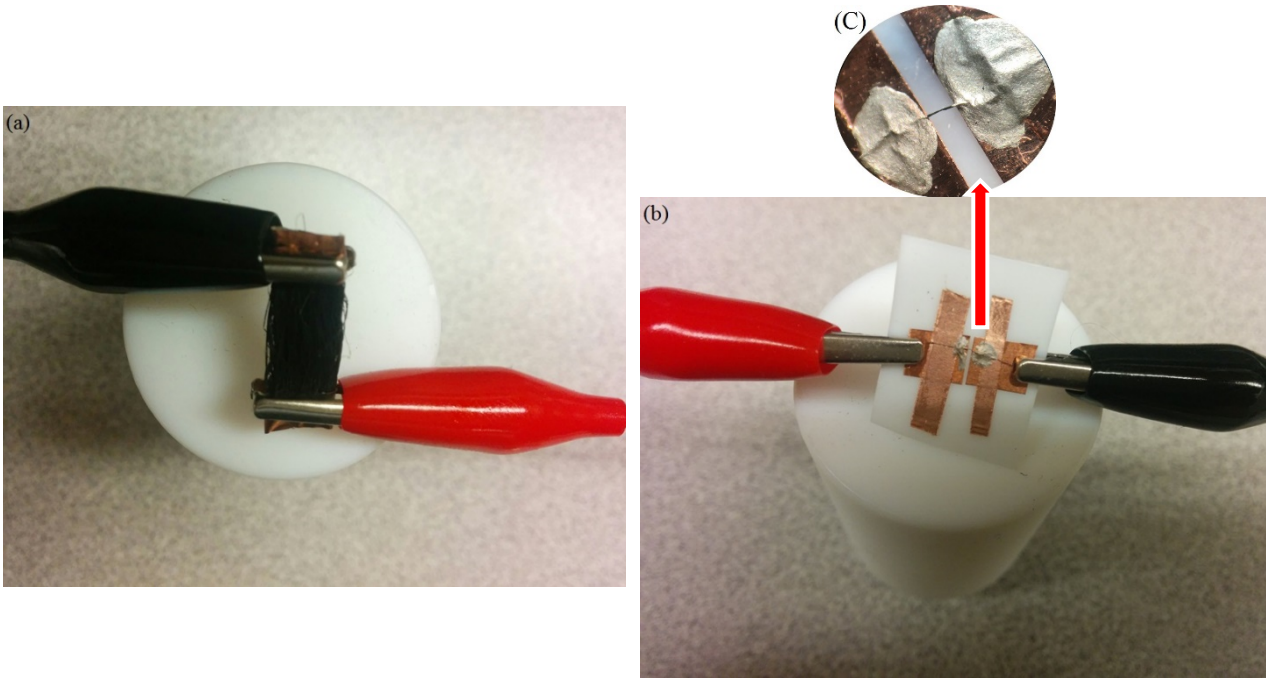

Figure 10. *Measuring the electrical resistance of (a) a 1000-fiber bundle and (b and c) a single fiber*

The conductivity of the composite fibers was measured based on a 1000-fiber bundle. As shown in **Figure 10 (a)**, the two ends of the fibers were connected with copper foil using conductive silver ink. Then, the specimen was connected with two electrodes of the Potentiostat (Princeton Applied Research, VersaSTAT 4). Three specimens were tested for each sample. In addition, as shown in **Figure 10 (b)** and **(c)**, the conductivity was also measured based on a single fiber. On the Teflon substrate, a single fiber was connected with the copper foil using

conductive silver ink. The electrodes of the Potentiostat were connected with the copper foil. Five specimens were tested for each sample. The current was measured while applied voltage increased from -10V to +10V using the Potentiostat (Princeton Applied Research, VersaSTAT 4). Linear regression was used for the voltage and current to calculate the resistance. The conductivity of the fibers (ρ) was calculated based on the measured resistance (R), length (L), and cross-sectional area (A) with the following equation.

$$\rho = \frac{RA}{L}$$

A single fiber with a gauge length of 10 mm was used for the measurement of the tensile properties based on ASTM Standard D3822/D3822M-14 using Instron Universal Testing Machine (Model 5560, Instron Engineering Corp., Canon, MA). For all of the tests, a 10 N loading cell was used. The extension rate was set to 24 mm/min, and 20 specimens were tested for each sample.

4.2 Results and Discussion

4.2.1 Morphology

The SEM images of pure PCL fibers and 5% CNF/PCL composite fibers obtained with the sheath-to-core flow rate ratio of 50:10 μL/min are shown in **Figure 11**. The incorporation of CNF into PCL changes the morphology of the fibers significantly. While pure PCL fibers exhibit smooth surfaces and uniform diameter along the longitudinal direction, the CNF/PCL composite fibers have a significantly higher surface roughness. The increase in surface roughness was expected because the CNFs decrease the uniformity of the pure PCL solution, which results in the fabrication of fibers with high surface roughness.

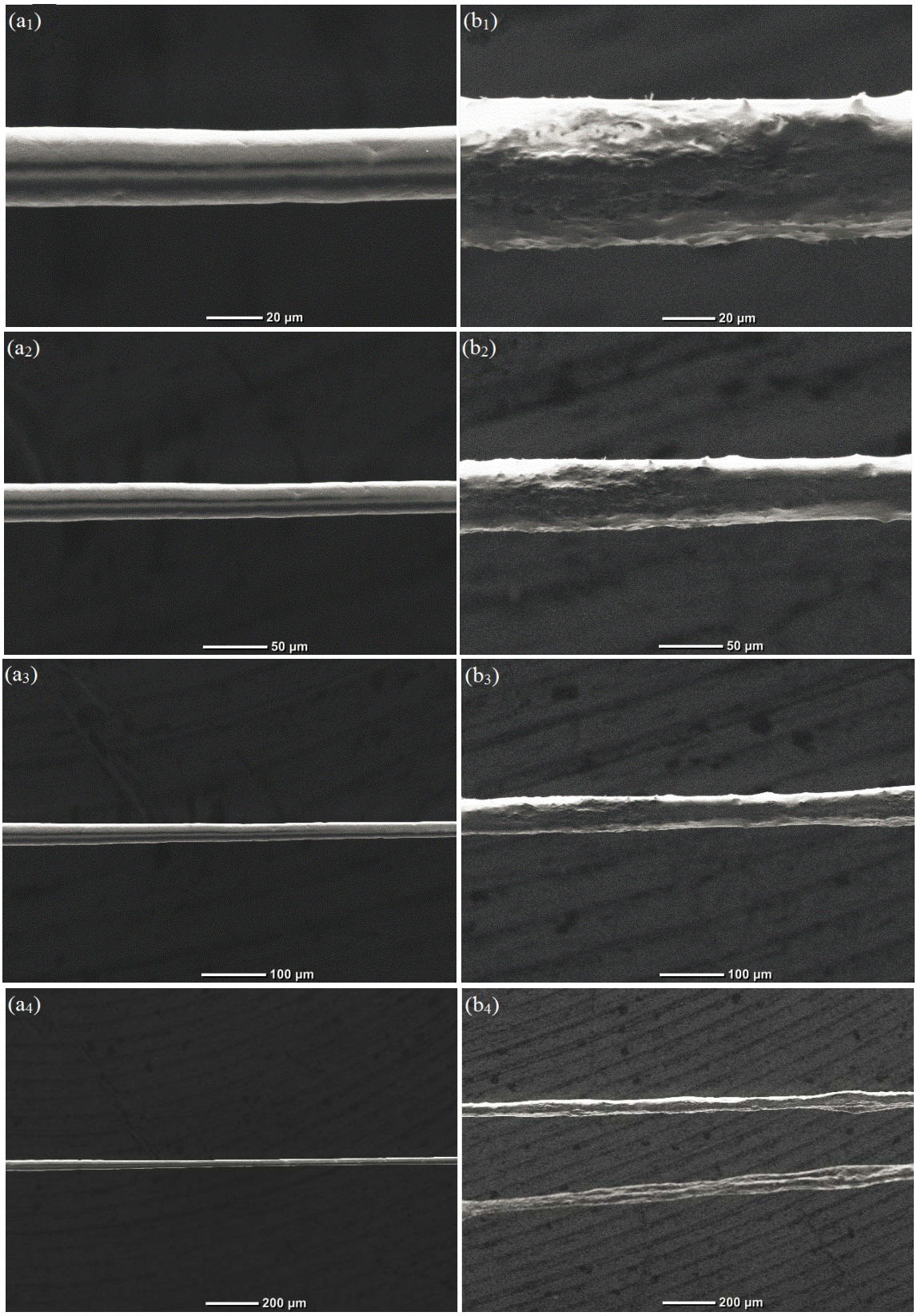

Figure 11. SEM Images of (a_1-a4) PCL and (b1-b4) 5 wt.% CNF/PCL composite fibers

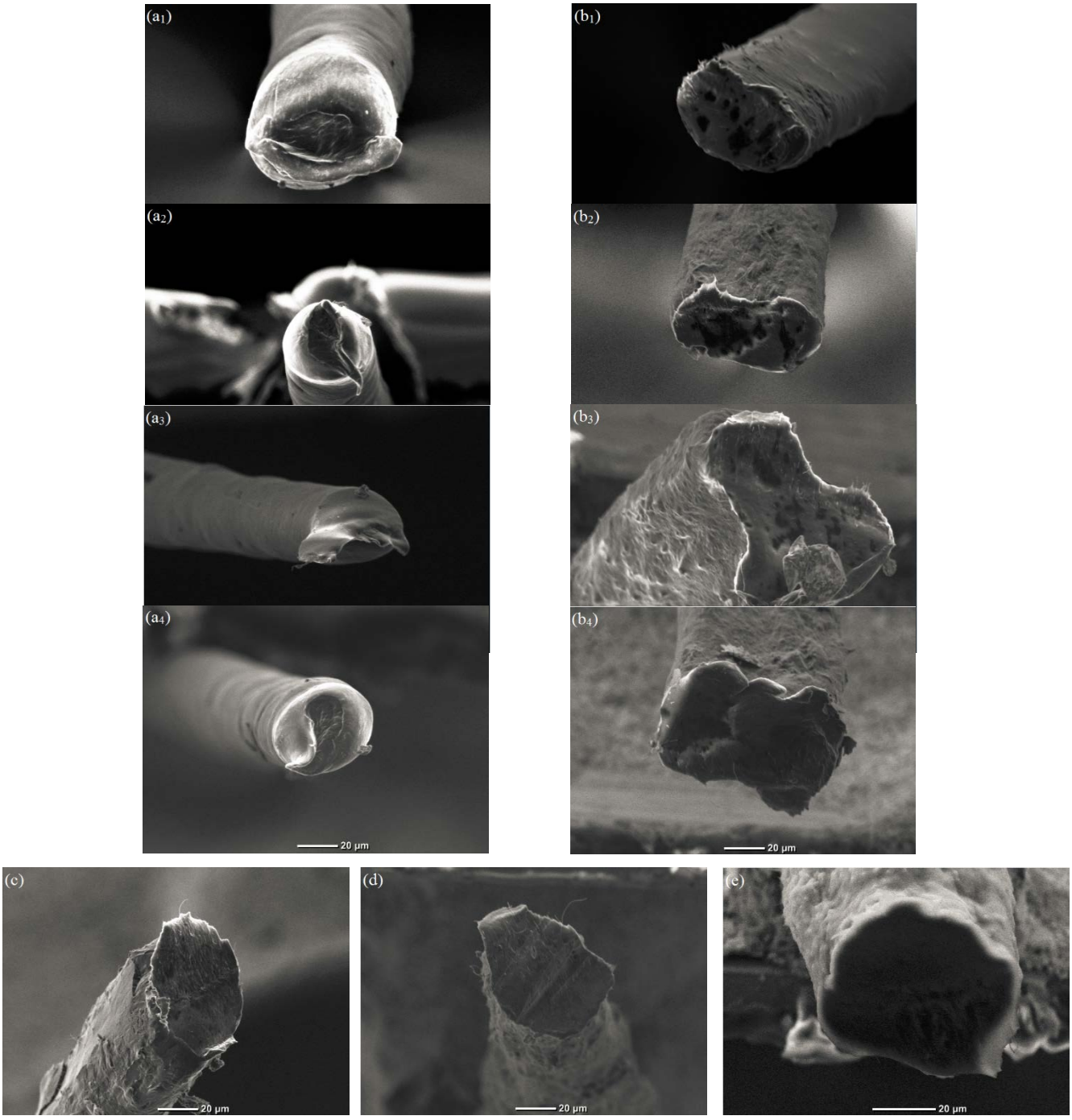

Figure 12. *Cross-sectional SEM images of (a1-a4) PCL fibers (sheath-to-core flow rate ratio: a_1-a_4: 50:10, 40:10, 30:10, 20:10, respectively), (b) 2.5 wt.% CNF/PCL fibers(b_1-b_4: 50:10, 40:10, 30:10, 20:10, respectively). (c) 3 wt.% CNF/PCL(50:10), (d) 4 wt.% CNF/PCL(50:10), and (e) 5 wt.% CNF/PCL(50:10)*

Additionally, the uniformity of the fiber diameter decreased which might due to the non-uniform dispersion of the CNFs in the core flow solution.

Furthermore, the addition of CNF increases the viscosity of the core fluid. A higher viscosity of the core flow results in a weakened hydrodynamic focusing from the sheath flow. Thus, the width of the core fluid in the channel increases, hence the resulting CNF/PCL composite fibers will have larger dimensions.

As shown in **Figure 12**, a higher flow rate ratio tended to give a more circular cross-sectional shape, and the addition of CNFs increased the cross-sectional area of the fibers.

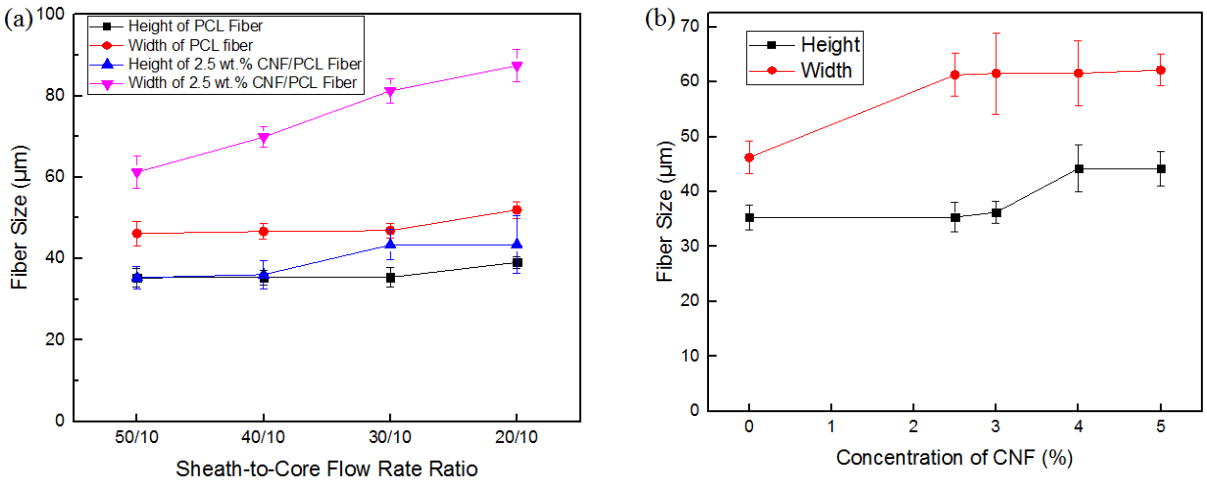

Figure 13. *Dimensions of fibers with (a) pure PCL and 2.5 wt.% CNF/PCL made with different sheath-to-core flow rate ratios. (b) Fibers with different concentrations of CNF made with sheath-to-core flow rate ratio of 50/10.*

Detailed dimensions of fibers with different concentration of CNFs and different flow rate ratios are shown in **Figure 13 (a)** and **(b)**. For pure PCL fibers, the height increased from 35.32 μm to 39.1 μm and width increased from 46.22 μm to 52.01 μm when the flow rate ratio

decreased from 50:10 to 20:10. Moreover, the aspect ratio slightly increased from 1.31 to 1.33. For 2.5 wt.% CNF/PCL fibers, the dimension changes more radically with changes in the flow rate ratio compared with pure PCL fibers. As the flow rate ratio decreased from 50:10 to 20:10, the height, width and aspect ratio increased from 35.36 µm to 43.50 µm, 61.25 µm to 87.44 µm and 1.73 to2.01,, and respectively. Additionally, the height, width and aspect ratio of fibers made with a flow rate ratio of 50:10 increased from 35.32 µm 44.2 µm , 46.22 µm to 62.13 µm and 1.31 to 1.41 respectively as the concentration of CNF increased from 0 wt.% to 5 wt.%. The change in morphology and size of the fibers is likely due to the weakened hydrodynamic focusing caused by increased core fluid and a smaller flow rate ratio.

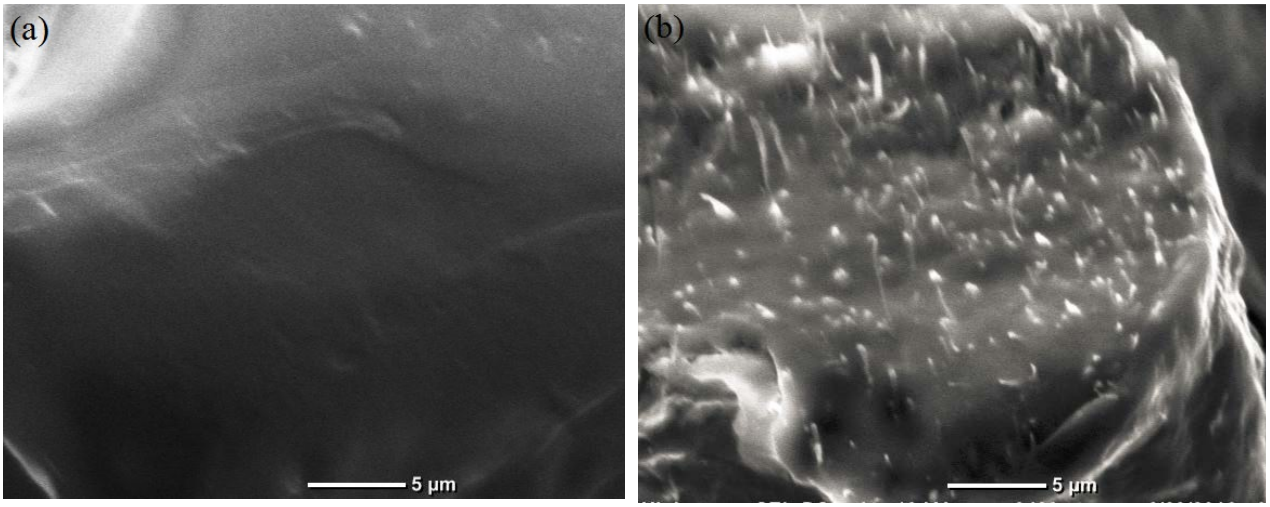

Figure 14. *Cross-sectional SEM images of (a) PCL fiber and (b) 5% wt.% CNF/PCL composite fiber made from flow rate ratio of 50/10*

Figure 14 shows the cross-sectional SEM image of the pure PCL fiber and CNF/PCL composite fibers with higher magnification. Compared to the smooth section of the PCL fiber, the cross-section of the CNF/PCL composite fiber exhibits high surface roughness as a result of

CNFs protruding out along the longitudinal direction of the fiber. The protruded CNFs provide evidence for their alignment along the longitudinal direction. The alignment of the CNFs could be explained as follows [3]: As the velocity of the flow in the channel distributes parabolically, the flow undergoes a shear force and its magnitude is a function of the distance from the walls of the microchannel. As the aspect ratio of the CNFs is significantly larger than 1, the CNFs could have a tendency of alignment due to the shear force. Before the conjunction of the core and sheath flows, the core fluid experiences a shear in the rectangular channel. Based on the distribution of the fluid velocity, a smaller distance from the microchannel walls results in larger shear rates due to the high velocity gradient. Although the shear rate is smaller because of the smaller core flow rate, it takes more time for the core flow to pass the relatively long inlet channel, which makes this part play an important role for the alignment of the CNFs. During hydrodynamic focusing, the core flow would be accelerated to match the speed of the sheath flow. As the core fluid spans the microchannel in the vertical direction at a location before the chevron grooves, the speed of the core flow along the vertical direction still possesses non-uniformity, which could also lead to shear forces. While the core fluid passes the pre-chevron groove region faster, accelerated core flow would result in larger shear rates. In addition, the elongational flows generated by hydrodynamic focusing could contribute to the alignment of the CNFs.

4.2.2 Electrical conductivity

Linear regression of current and voltage were performed in R Language to obtain the resistance. Acceptable linearity between Current and Voltage were found with a coefficient of determination R^2 larger than 0.98. Typical Current-Voltage fitting lines are shown in **Figure 15**.

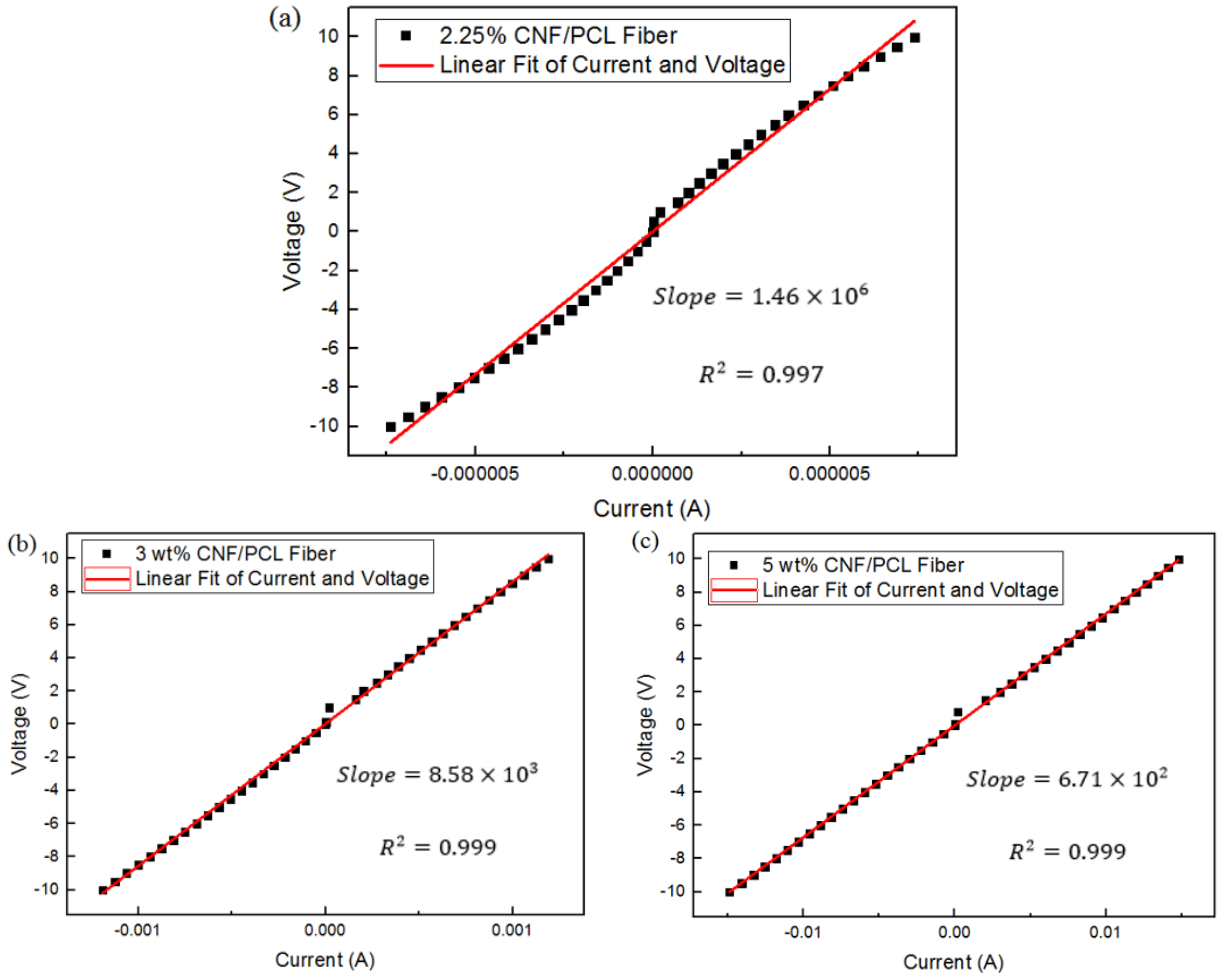

Figure 15. *Current-Voltage data and fitting lines of the 1000-fiber bundle samples with CNF content of (a) 2.25 wt.%, (b) 3wt.%, and (c) 5 wt.%.*

CNF/PCL composite fibers exhibited non-continuous conductivity as the concentration of the CNFs were lower than 3 wt.%. This lead to the conductivity of the single-fiber specimens to be tested only with CNF concentrations higher than 3wt.%.

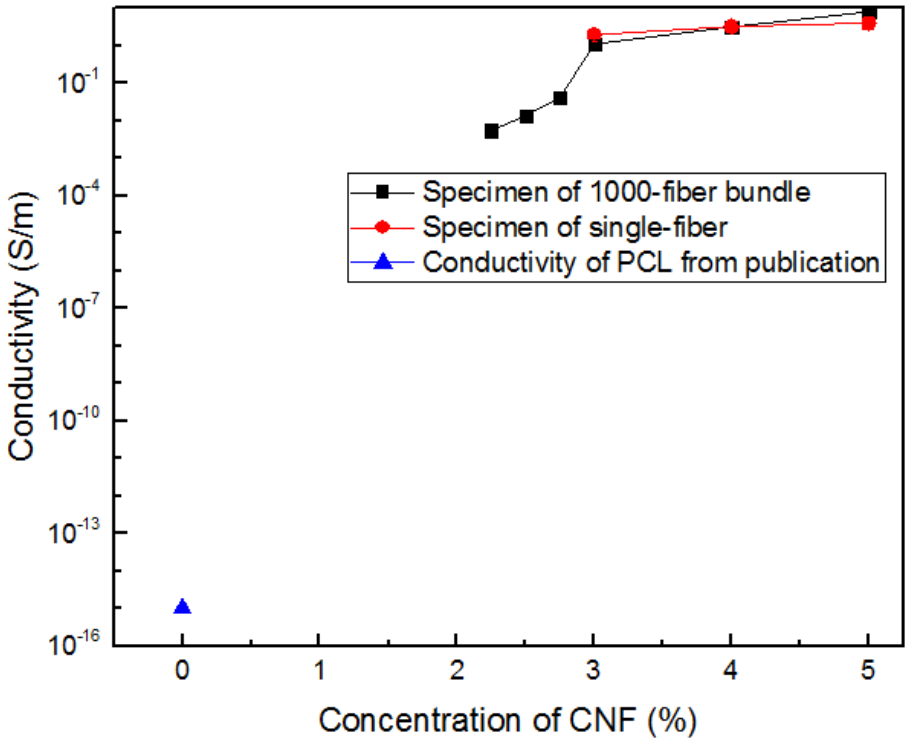

Figure 16. *Conductivity of fibers as a function of CNF concentration*

Figure 16 shows the change of the electrical conductivity of the CNF/PCL fibers as a function of CNF concentration. The resistance of the composite fibers reached detectable levels as the concentration of CNFs increased to 2.25 wt.%. Originally, the conductivity of the composite fibers increased significantly with the increasing of CNFs concentration.

Table 3. *Conductivity of Composite fibers with different CNF concentration (sheath-to-core flow rate ratio=50/10)*

Weight ratio(CNF/PCL)	2.25/100	2.5/100	2.75/100	3/100	4/100	5/100
Conductivity (S/m) (measured based on 1000-fiber bundle)	(5.47±1.25) $\times 10^{-3}$	(1.36±0.15) $\times 10^{-2}$	(4.20±0.75) $\times 10^{-2}$	1.11± 0.28	3.19± 0.65	8.02± 1.50
Conductivity(S/m) (measured based on single fiber)	---	---	---	1.96± 0.41	3.27± 0.77	4.02± 1.19

As shown in **Table 3**, the electrical conductivity increased from 5.47×10^{-3} to 1.11 S/m while the concentration of CNFs increased from 2.25 wt.% to 3 wt.%. Compared with the conductivity of PCL, which is approximately 10^{-15} S/m [4], there was an increase by an order of 10^{15}. As the concentration of CNFs reached 3 wt.%, the rate of increasing conductivity decreased. Rising the concentration of the CNFs from 3 wt.% to 5 wt.%, the conductivity increased slightly from 1.11 to 8.02 S/m based on the 1000-fiber bundle specimen and from 1.96 to 4.02 S/m based on the single-fiber specimen. In addition, the conductivity values which were measured based on the 1000-fiber bundle and single-fiber specimen were comparatively close, which provided evidence for the continuity of conductivity.

Table 4. *Percentage of resistance-undetectable of 2.5 wt.% CNF/PCL fibers*

Sheath-to-Core Flow Rate Ratio	50/10	40/10	30/10	20/10
Percentage of Undetectable Samples	4/10	4/10	2/10	1/10

In order to investigate the continuity of conductivity, 10 single-fiber samples of 2.5 wt.% CNF/PCL composite fibers from different flow rate ratios were measured using a digital multi-meter. As shown in **Table 4**, a lower flow rate ratio shows more continuous conductivity.

Table 5. *Conductivity of Composite fibers fabricated by using different flow rate ratios*

Flow Rate Ratio (sheath flow/core flow)	50/10	40/10	30/10	20/10
Conductivity of 2.5 wt.% CNF/PCL Fiber (S/m) (measured based on 1000-fiber bundle)	$(1.36\pm0.15)\times10^{-2}$	$(5.31\pm1.38)\times10^{-2}$	$(1.28\pm0.18)\times10^{-1}$	$(5.97\pm1.42)\times10^{-2}$
Conductivity (S/m) 5 wt.% CNF/PCL Fiber (S/m) (measured based on single fibers)	4.02±1.19	3.09±0.38	2.93±0.73	2.63±0.50

The conductivity of 2.5 wt.% CNF/PCL composite fibers measured based on the bundle of 1000 fibers is shown **Table 5**.

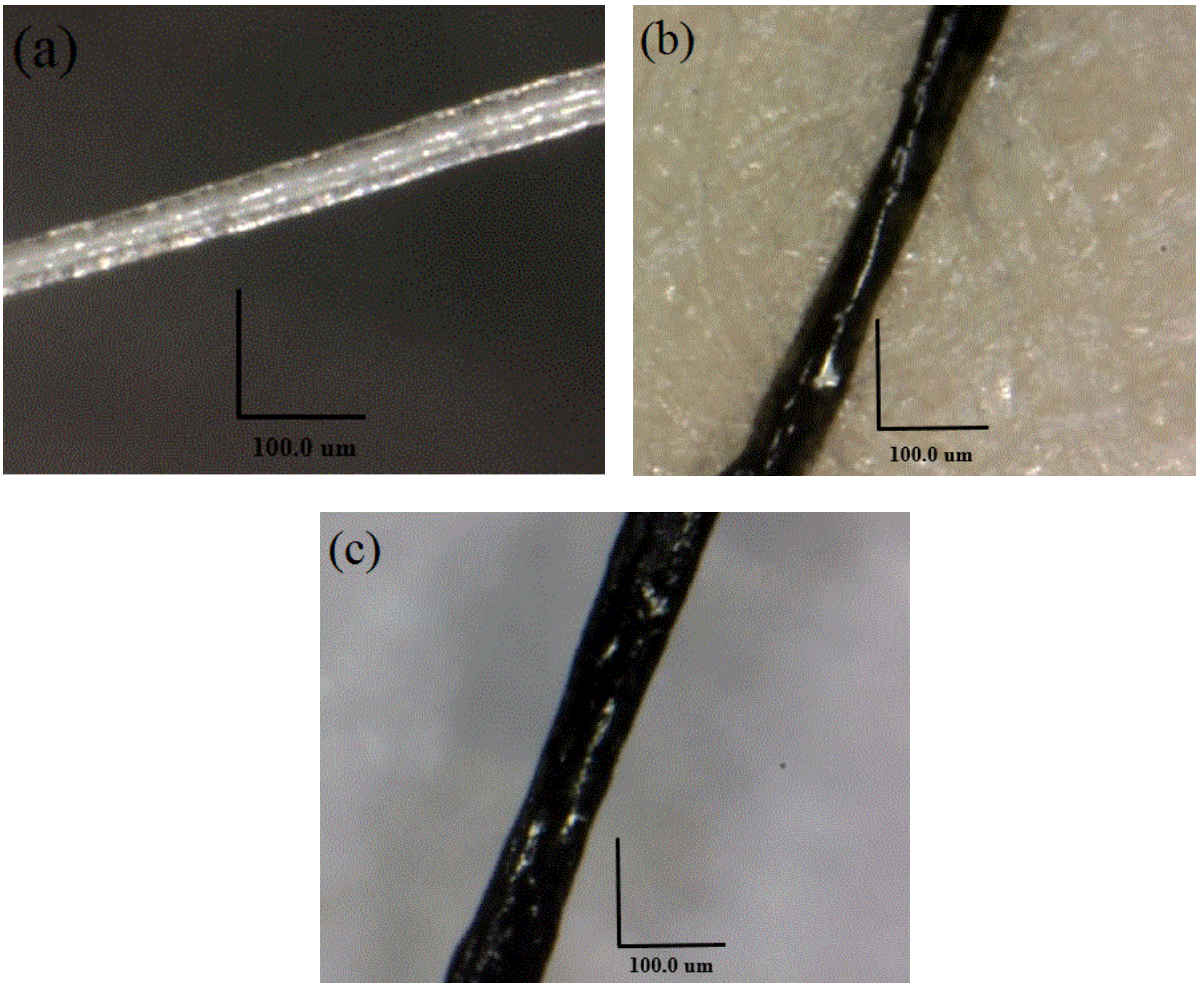

Figure 17. *Microscopic Images of (a) pure PCL, (b) 2.5 wt.% CNF/PCL, and(c) 3% wt.% CNF/PCL fibers fabricated with sheath-to-core flow rate ratio of 50/10*

Figure 17 depicts the optical microscope images of pure PCL fiber, 2.5 wt.% CNF/PCL fiber, and 3 wt.% CNF/PCL fiber. The pure PCL fibers were white and semi-transparent and the color changed to dark while the transparency decreased as PCL incorporated with CNFs. For 2.5 wt.% CNF/PCL fiber, some discontinuous and partially CNF-filled PCL regions were observed. As the concentration of CNF increased to 3 wt.%, no discontinuous region was found. For the 2.5 wt.% CNF/PCL fiber, the CNFs were not enough to fully fill the PCL matrix, which led to a

non-continuous distribution and low conductivity. For a lower flow rate ratio, the core flow would take more space in the microchannel, which would result in fibers with larger cross-sectional areas. This suggests that the probability of the conductivity discontinuity might be decreased. On the other hand, a higher flow rate ratio produced larger shear forces during the hydrodynamic focusing, which aligns the CNFs along the fiber direction. The alignment of the CNFs is helpful for obtaining higher conductivity. These two competitive factors made the conductivity of 2.5 wt.% CNF/PCL 1000-fiber bundle increase from $(1.36\pm0.15)\times10^{-2}$ S/m at the sheath-to-core flow rate of 50/10 to $(1.28\pm0.18)\times10^{-1}$ S/m at the sheath-to-core flow rate of 30/10 and then decreased to $(5.97\pm1.42)\times10^{-2}$ S/m as the sheath-to-core flow rate ratio changed to 20/10 (as shown in **Figure 18** and **Table 5**).

Table 5 also shows the conductivity of 5 wt.% CNF/PCL composite fibers measured based on a single fiber. As the CNF concentration of 5 wt.% is high enough for producing continuous conductivity, the conductivity of the composite fiber is mainly determined by the alignment of the CNFs. As lower flow rate ratios resulted in smaller shear stress during the hydrodynamic focusing, the alignment of the CNFs was weakened. As a result, the conductivity of the composite fibers decreased from 4.02 S/m to 2.63 S/m when the flow rate ratio was decreased from 50:10 to 20:10 However, as the concentration of the CNFs already exceeded the percolation, the change of the conductivity was very small.

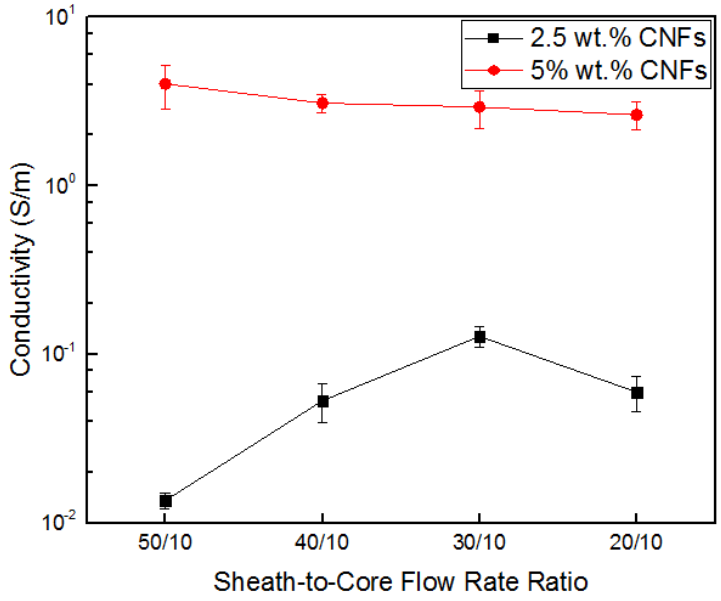

Figure 18. *Conductivity of fibers made by using different sheath-to-core flow rate ratios and CNF concentrations of 2.5 wt.% and 5 wt.%*

4.2.3 Tensile properties

Typical of the strain-stress curves for the PCL and PCL/CNF are shown in **Figure 19**. **Figure 19 (a)** shows strain-stress curves of fibers with different content of CNF. In this figure, at the beginning, the tensile strength of the fiber increased with increasing the concentration of CNFs. As the concentration of the CNFs reached 3 wt.%, the strength started decreasing by further increasing the CNFs concentration. That might be due to the voids produced by the agglomeration of the CNFs at a high concentration. **Figure 19 (b)** depicts the tensile strength of 2.5 wt.% CNF/PCL composite fibers fabricated with different flow rate ratios. This figure also demonstrates that a higher flow rate ratio tends to result in fibers with a higher strength. As mentioned in the previous section, a larger flow rate ratio would produce a larger shear rate during the hydrodynamic focusing, which would be helpful for aligning the CNFs as well as PCL

polymer chain along the fiber direction. This leads to the realization that increased tensile strength can be ascribed to the alignment of the CNFs.

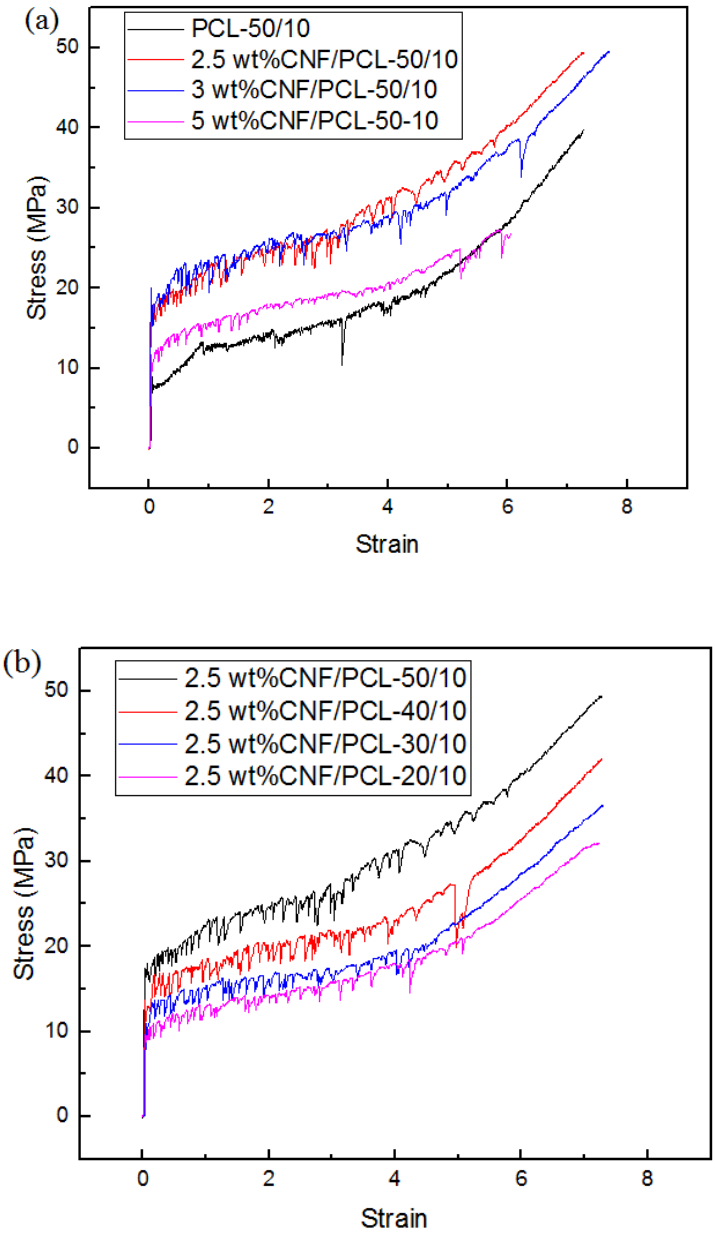

Figure 19. *Strain-stress curves of (a) fibers with different CNFs content and (b) fibers from different flow rate ratios*

Table 6. *Tensile Properties of PCL and CNF/PCL Fibers*

Weight ratio(CNF /PCL)	Flow Rate Ratio (sheath flow/core flow)	Yield strength (MPa)	Young's Modulus(MPa)	Failure strength(MPa)	Elongation at break
0/100	50/10	8.84±0.50	322.62±23.57	40.06±1.91	7.38±0.21
	40/10	9.26±0.43	334.26±13.96	41.59±1.72	7.35±0.09
	30/10	8.88±0.37	317.20±17.15	37.03±1.12	6.84±0.16
	20/10	7.69±0.52	287.60±15.99	29.79±1.55	6.54±0.18
2/100	50/10	11.69±0.40	606.68±23.34	43.35±2.00	7.42±0.23
2.5/100	50/10	14.05±0.32	820.19±35.82	48.19±1.43	7.57±0.18
	40/10	11.83±0.49	665.88±35.85	41.71±1.78	7.50±0.21
	30/10	10.89±0.30	594.76±22.50	36.95±1.31	7.20±0.17
	20/10	9.99±0.21	537.55±25.79	33.03±1.62	7.26±0.17
3/100	50/10	15.21±0.87	929.57±51.31	49.21±2.35	7.63±0.32
4/100	50/10	8.63±0.27	562.41±13.39	34.42±1.05	6.78±0.13
5/100	50/10	8.55±0.49	556.50±25.59	24.11±1.37	4.96±0.45

The detailed tensile properties of the PCL and CNF/PCL fibers are provided in **Table 6**. For the PCL fibers, the tensile strength had a tendency of increasing and then decreasing as the sheath to core flow rate ratio increased. Two competitive factors may play a role for the change of the tensile strength with the flow rate ratio. For higher flow rate ratios, the resulting fibers have smaller cross-sectional areas which indicates the occurrence probability of voids is smaller. The failure of material starts from the voids and then the propagation of cracks finally leads to the breaking-down of the material. Owing to smaller occurrence probability of voids could be endowed by higher flow rate ratios, fibers fabricated with higher flow rate ratio show higher tensile strength. However, decreasing the flow rate ratio could increase the aspect ratio of the fibers, which was demonstrated to endow fibers with higher strength [2]. As shown in **Section 3.1**, because the change of aspect ratio is very small, the decreasing of the cross-sectional area might play a more important role. For the samples with the CNF concentration of 2.5 wt.%, the yield strength, Young's Modulus and ultimate strength of the fibers fabricated with the sheath-to-core flow rate ratio of 50:10 were 1.41, 1.53 and 1.46 times of fibers fabricated with the flow rate ratio of 20:10, respectively. The addition of CNFs with a concentration of 3 wt.% resulted in the maximum tensile strength. The yield strength, Young's Modulus, and ultimate strength of 3 wt.% CNF/PCL composite fiber were 15.21 MPa, 929.57 MPa and 49.21 MPa, which were respectively 1.72, 2.88 and 1.23 times of the pure PCL fiber.

4.3 Reference

[1] Z. Bai, J.M.M. Reyes, R. Montazami, N. Hashemi, Journal of Materials Chemistry A, 2 (2014) 4878-4884.

[2] F. Sharifi, D. Kurteshi, N. Hashemi, Journal of the Mechanical Behavior of Biomedical Materials, 61 (2016) 530-540.

[3] A.R. Shields, C.M. Spillmann, J. Naciri, P.B. Howell, A.L. Thangawng, F.S. Ligler, Soft Matter, 8 (2012) 6656-6660.

[4] S.J. Chin, S. Vempati, P. Dawson, M. Knite, A. Linarts, K. Ozols, T. McNally, Polymer, 58 (2015) 209-221.

CHAPTER 5
CONCLUSION AND FUTURE WORK

5.1 Conclusion

A cross-flow geometry microfluidic with one inlet for core flow and two inlets for sheath flow was designed for microfluidic fiber fabrication. After the conjunction of the core flow and sheath flow, four chevron-shaped grooves as shaping elements were built on the ceiling and bottom of the microchannel. A CNC micro-milling machine was used to create the PMMA master molds, the surfaces of which were further finished by chloroform vapor. PDMS microchannel was prepared by molding replication based on the micro-machined PMMA master molds. Using the as-fabricated PDMS microchannel, electrically conductive CNF/PCL composite fibers were successfully fabricated using the microfluidic method. The morphology, electrical conductivity, and tensile strength were investigated as a function of sheath-to-core flow rate ratios and content of carbon nanofibers. The results showed that the microfluidic method is a viable approach for aligning the CNFs along the longitudinal direction of the fibers. The orientation of the CNFs showed a positive effect on the electrical conductivity and tensile strength. The yield strength, Young's Modulus and ultimate strength of the fibers fabricated with the flow rate ratio of 50/10 were 1.41, 1.53 and 1.46 times of fibers fabricated with the flow rate ratio of 20/10. The tensile strength of the composite fibers reached the maximum at 3 wt.%. For the 3 wt.% CNF/PCL composite fiber the electrical conductivity was 1.11 S/m. The yield strength, Young's Modulus and ultimate strength of the composite fiber was 1.72, 2.88 and 1.23 times of pure fiber. Further increasing the content of CNFs, the electrical conductivity increased slightly, while the tensile strength dropped sharply due to the agglomeration of CNFs.

5.2 Future work

In order to further increase the electrical conductivity of the CNF/PCL composite fiber, retain fairly strong mechanical strength, and dimension uniformity of the fiber, chemical modification of the CNF surface or surfactant might be needed to improve the dispersion of carbon nanofiber in the PCL matrix and enhance the efficiency of stress transfer between PCL matrix and CNFs.

In addition, instead of using one type of conductive filler, the mixture of conductive fillers with different size, shape and aspect ratio might be able to facilitate the formation of the conductive network in the polymer matrix and decrease the percolation threshold[1].

What's more, although 15% PEG was added into the sheath solution to increase the viscosity, the viscosity of the sheath solution was still lower than that of the core solution. More work might be needed to investigate the influence of sheath solution viscosity on the properties of resulting fibers.

Besides, as PCL is one kind of crystallizable polymer, the conductive fillers might be able to play a role as nucleation for crystal growth. The properties of the polymer might be greatly affected by the percent of crystallinity. So the influence of conductive fillers on the crystallization of PCL matrix might need to be studied.

Owing to the increased electrical conductivity, electrical signals could pass through the fiber more efficiently. Other kinds of functional materials, like electrochromic materials[2], could be incorporated into the composite fiber to fabricate smart fibers initiated by electrical signals.

Owing to its biocompatibility, PCL was chosen as the polymer matrix in this thesis to work to fabricate electrical conductive composite fiber that could be used in biological areas.

However, the low glass transition temperature (about 60 ˚), small yield strain and hydrophobicity might restrict its application in more fields. As mentioned in previous sections, the microfluidic fiber fabrication approach possesses high versatility and flexibility, other polymer matrix with different properties could be used as needed to fabricate electrical conductivity fibers.

5.3 References

[1] R. Ma, J. Lee, D. Choi, H. Moon, S. Baik, Nano Letters, 14 (2014) 1944-1951.

[2] S.Y. Jang, V. Seshadri, M.S. Khil, A. Kumar, M. Marquez, P.T. Mather, G.A. Sotzing, Advanced Materials, 17 (2005) 2177-2180.